# DATA BASE GENERATION FOR VARIABLE INFILTRATION CAPACITY (VIC) HYDROLOGIC BASED MODEL - REMOTE SENSING AND GIS APPROACH

**M. Tech. (Agril. Engg.) THESIS**

**By**

**SHASHI KANT**

**DEPARTMENT OF SOIL AND WATER ENGINEERING**

**FACULTY OF AGRICULTURAL ENGINEERING**

**INDIRA GANDHI AGRICULTURAL UNIVERSITY**

**RAIPUR (C.G.)**

**2005**

# DATA BASE GENERATION FOR VARIABLE INFILTRATION CAPACITY (VIC) HYDROLOGIC BASED MODEL - REMOTE SENSING AND GIS APPROACH

*Thesis*

**Submitted to the**

**Indira Gandhi Agricultural University, Raipur**

**By**

**SHASHI KANT**

**IN PARTIAL FULFILMENT OF THE**

**REQUIREMENTS FOR THE**

**DEGREE OF**

**Master of Technology**

**in**

**Agricultural Engineering**

**(Soil and Water Engineering)**

**Roll No: 3279** **ID NO: PG/Agril.Engg./2003/08**

**OCTOBER, 2005**

# CERTIFICATE – I

This is to certify that the thesis entitled **"Water Balance Studies of a Micro Watershed"** submitted in partial fulfillment of the requirements for the degree of "Master of Technology in Agricultural Engineering" of the Indira Gandhi Krishi Vishwavidyalaya, Raipur, is a record of the bonafied research work carried out by **Shri Johnson K. Eappen** under my guidance and supervision. The subject of the thesis has been approved by the Student's Advisory Committee and the Director of Instructions.

No part of the thesis has been submitted for any other degree or diploma (certificate awarded *etc.*) or has been published/published part has been fully acknowledged. All the assistance and help received during the course of the investigations have been duly acknowledged by him.

Date: **Chairman**

**THESIS APPROVED BY THE STUDENT'S ADVISORY COMMITTEE**

Advisory Committee

| | | |
|---|---|---|
| Chairman | (Dr. M. P. Tripathi) | ---------- |
| Member | (Dr. R. K. Sahu) | ---------- |
| Member | (Dr. V. K. Pandey) | ---------- |
| Member | (Dr. A. P. Singh) | ---------- |
| Member | (Dr. S. S. Tuteja) | ---------- |

# CERTIFICATE – II

This is to certify that the thesis entitled **"Data Base Generation for Variable Infiltration Capacity (VIC) Hydrologic Based Model - Remote Sensing and GIS Approach"** submitted by **Shri Shashi Kant** to the Indira Gandhi Krishi Vishwavidyalaya, Raipur in partial fulfillment of the requirements for the degree of **M. Tech. (Agril. Engg.)** in the Department of **Soil and Water Engineering** has been approved by the Student's Advisory Committee after oral examination in collaboration with the external examiner.

External Examiner

Major Advisor

Head of the Department

Director of Instructions

Date:

# *Acknowledgements*

*To GOD be all the glory great things he has done. All my sincere gratitude goes to him for the help he has given me and his unfailing mercies over my life he has been kind to me.*

*I wish to express my deep sense of respect and indebtedness to my major adviser Dr. M. P. Tripathi, Associate Professor, Department of Soil and Water Engineering, Faculty of Agricultural Engineering, I. G. A. U., Raipur, for his valuable, talented, inspiring, constructive criticism, and ceaseless encouragement provided during the entire project work.*

*Indeed the words at my command are not adequate, either in form of sprit, to convey the depth of my feelings of gratitude to my co-advisor Dr. V. Hari Prasad Head, Water Resource Divison, IIRS, Dehradun , for his most valuable guidance , suggestions, useful critisism and whole hearted support during the study with his ever smiling face.*

*I am very thankful to senior member of my advisory committee Dr. R. K. Sahu, Dean and Head of the Department of Soil and Water Engineering, Faculty of Agricultural Engineering, I. G. A. U., Raipur, for his constant encouragement during project completion.*

*I have a great pleasure in expressing my sincere thanks to my advisory committee members, Dr. V. K. Pandey, Dr. V. P. Verma and Er. A. P. Mukharjee for their priceless guidance, worthy suggestions and constant encouragement throughout the project.*

*I am extremely thankful to, Dr.S.P Agrawal and Er,Praveen Thakur ,Water Resource Divison, IIRS, Dehradun apart from all the members of Faculty of Agricultural Engineering including Er. S. B. Yadav, Dr. B. P. Mishra, Dr. S. Patel, Er. M. Quasim, Er. S. V. Jogdand, Er. A. K. Dave, Er. A. K. Pali, Er. A. K. Verma, Er. M. Victor, Er. J. Nikhade, and Er. P. K. Katre for their time to time co-operation during the course of study.*

*I am thankful to all the staff members of Faculty of Agricultural Engineering for their kind support and help at various stages of the study.*

*I avail this pleasant opportunity to express my sincere thanks to all of my friend, Johnson ,Sam, Pavitra,Abhishek, Sunil, Prakash, Sachin, Nitin, Tushar, Anand, vivek, Sachin, Manoj, Dheeraj,Baljeet, Shrilatha, Saisudha, Renu, and all of my other friends for their love, contribution and timely help during course of study. Also I express special thanks to all those who helped directly or indirectly during this study.*

*My literacy power is too less to express my gratitude to Dr. C. R. Hazra, Hon'ble Vice Chancellor, Dr. M. N. Shrivastava, Director of Research Services and Dr. S. N. Puri, Director of Instruction, I.G.A.U., Raipur for providing necessary facilities for conducting the project.*

*Last but not least, words runs short to express my heartfelt gratitude to my beloved parents and my family membersfor their boundness, generosity, inspiration, encouragements everlasting blessing and abundant love for me for successful completion of this achievement.*

*Place: Raipur* *( Shashi Kant )*

*Date:*

# CONTENTS


| Sl. No. | Caption | Page No. |
|---|---|---|
| | **Acknowledgements** | i-ii |
| | **List of Tables** | iii |
| | **List of Figures** | iv |
| | **List of Plates** | v |
| | **List of Abbreviations** | vi |
| | **List of Symbols** | vii |
| | **Abstract** | viii |
| **I** | **Introduction** | |
| **II** | **Review of Literature** | |
| 2.0 | Applications of Remote Sensing and GIS | |
| 2.1 | Remote Sensing in Hydrology | |
| 2.2 | Application of GIS in Hydrology | |
| 2.2.1 | Use of GIS | |
| 2.2.2 | Integration of GIS and Remote Sensing in Hydrological Modeling | |
| 2.2.3 | Data extraction from DEM/DTM | |
| 2.2.4 | Ground and Surface Water Interaction | |
| 2.3 | Concepts and Classification of Models | |
| 2.4 | Variable Infiltration Capacity (VIC) Model | |
| 2.4.1 | VIC model in PILP Project | |
| **III** | **Materials and Methods** | |
| 3.1 | The Study Area | |
| 3.2 | Hardware and the software used | |
| 3.3 | Data Acquisition | |
| 3.3.1 | USGS GTOPO30 elevation data | |
| 3.3.2 | MM5 V3 terrain data | |
| 3.3.3 | Land use/land cover data of south central Asia | |
| 3.3.4 | LDAS information | |

3.4 VIC-2L Model Overview
3.5 Projection System used for the Datasets
3.6 Raster Grid Map Generation
3.7 Soil Dataset Generation
3.7.1 Derivation of Soil texture data at model grid resolution
3.7.2 Soil Parameters
3.7.3 Generation of raster attribute maps for the soil parameters
3.8 Vegetation data set
3.8.1 Derivation of land use/cover data
3.8.2 Vegetation parameters
3.8.3 Generation of raster data for the vegetation parameters
3.9 Topographic dataset generation
3.9.1 DEM extraction from GTOPO 30 data
3.9.2 Slope Generation from the raster DEM
**IV Results and Discussion**
4.1 Topographic Dataset
4.2 Generation of Digital Soil Datasets
4.2.1 Extraction of soil texture data
4.2.2 Soil Parameters
4.3 Derivation of Land use/ cover data
4.3.1 Vegetation Parameters
**V Summary and Conclusions**
**Suggestions for Future Research Work**
**Bibliography**
**Appendices**

# LIST OF TABLES


| Table No. | Caption | Page No. |
|---|---|---|
| 3.1 | The corner pixel information of generated raster grid map | |
| 3.2 | The Untarred files of *MM5 V3 Terrain* data | |
| 3.3 | Band information of MM5 V3 Terrain data | |
| 3.4 | Samples and Line values for subseting the soil data | |
| 3.5 | Lines and sample values of subset image corresponding to raster grid map | |
| 3.6 | GCPs used for georeferencing soil data in Albers conical projection | |
| 3.7 | GTOPO 30 tiles used for DEM extraction | |
| 3.8 | Terrain scenes produced using *3dem* software | |
| 3.9 | Corner position of mosiacked image used for georeferencing | |
| 4.1 | Pixels distribution of the DEM data | |
| 4.2 | Pixel distribution of soil texture data | |
| 4.3 | Pixel distribution of Brook's Corey Exponent parameter | |
| 4.4 | Pixel distribution of saturated hydraulic conductivity | |
| 4.5 | Pixel Distribution of soil particle density of the soil layers | |
| 4.6 | Soil bulk density parameter | |
| 4.7 | Fractional soil moisture content at critical point | |
| 4.8 | Fractional soil moisture content at wilting point | |
| 4.9 | Pixel distribution of residual moisture fraction | |
| 4.10 | UMD vegetation classes in assimilated Land use/cover data | |
| 4.11 | Spatial variation of average monthly LAI values for UMD vegetation class | |

4.12 Spatial variation of average monthly RL values for UMD vegetation class

4.13 Spatial variation of average monthly VHD values for UMD vegetation class

4.14 Spatial distribution of architectural, stomatal resistance and rooting depth

## LIST OF FIGURES


| Figure No. | Caption | Page No. |
|---|---|---|
| 3.1 | Variable Infiltration Curve-2Layer Model (VIC-2L) | |
| 4.1 | Pixel distribution with respect to the elevation range of the DEM | |
| 4.2 | Spatial variation of soil texture data | |

# LIST OF PLATES


| Plate No. | Title | Page No. |
|---|---|---|
| 3.1 | Global USGS GTOPO 30 DEM data | |
| 3.2 | Tiles of GTOPO 30 data used for DEM extraction during study | |
| 4.1 | Extracted DEM from GTOPO 30 data for the study area | |
| 4.2 | Slope map (%) derived for the study area from the extracted DEM | |
| 4.3 | Soil texture map of upper soil layer (0-30 cm depth) | |
| 4.4 | Soil texture map of lower layer depth (30-100cm) | |
| 4.5 | Brook's Corey Exponent parameter | |
| 4.6 | Saturated hydraulic conductivity (mm/day) | |
| 4.7 | Soil particle density parameter ($kg/m^3$) | |
| 4.8 | Soil bulk density parameter ($kg/m^3$) of soil layers | |
| 4.9 | Fractional soil moisture content at critical point (*Wcr_Fract)*) | |
| 4.10 | Fractional soil moisture content at wilting point (*Wpwp_Fract*) | |
| 4.11 | Residual moisture fraction parameter | |
| 4.12 | Landuse/cover map for UMD vegetation classes | |
| 4.13 | LAI values for the month of June and December | |
| 4.14 | RL values for the month of June and December | |
| 4.15 | Vegetation displacement height for June and December | |
| 4.16 | Minimum stomatal resistance in [sec $m^{-1}$] | |
| 4.17 | Architectural resistance in [sec $m^{-1}$] | |

# LIST OF ABBREVIATIONS

| Abbreviation | Description |
|---|---|
| Agri. | Agriculture |
| Agril. Engg. | Agricultural Engineering |
| ALMA | Assistance for Land-surface Modeling Activities |
| API | Application Programming Interface |
| AVHRR | Advanced Very High Resolution Radiometer |
| BMRC | Bureau of Meteorology Research Center |
| BRDF | Bidirectional Reflectance Distribution Function |
| CGI | Common Gateway Interface |
| CLM | Community Land Model |
| DAAC | Distributed Active Archive Center |
| DEM | Digital Elevation Model |
| DIS | Data Information System |
| DMSP | Defense Meteorological Satellite Program |
| DODS | Distributed Ocean Data System |
| Eq. | Equation |
| EROS | Earth Resources Observation Systems |
| ESMF | Earth System Modeling Framework |
| ESRI | Environmental Systems Resources Institute |
| ESSC | Earth System Science Center |
| FEMA | Federal Emergency Management Agency |
| FSU | Florida State University |
| FTP | File Transfer Protocol |
| GFDL | Geophysical Fluid Dynamics Laboratory |
| GIS | Geographical Information System |
| GOES | Geostationary Operational Environmental Satellite |
| GrADS | Grid Analysis and Display System |
| GRID | Global Resources Information Database |

| | |
|---|---|
| GSM | Global Spectral Model |
| ICAR | Indian Council of Agricultural Research |
| IGAU | Indira Gandhi Agricultural University |
| IGBP | International Geosphere-Biosphere Programme |
| ISRIC | International Soil Reference and Information Centre |
| JMA | Japan Meteorological Agency |
| LAI | Leaf Area Index |
| LAS | Land Analysis System |
| LDAS | Land Data Assimilation System |
| LIS | Land Information System |
| Lsm | land surface model |
| M. Tech. | Master of Technology |
| MM5 | Fifth Version of the Mesoscale Model |
| MRTG | Multi Router Traffic Grapher |
| MSL | Mean Sea Level |
| NASA | National Aeronautics and Space Administration |
| NCAR | National Center for Atmospheric Research |
| NCEP | National Centers for Environmental Prediction |
| NDVI | Normalized Difference Vegetation Index |
| NFS | Network File System |
| NHC | National Hurricane Center |
| NOAA | National Oceanic and Atmospheric Administration |
| NRCS | Natural Resources Conservation Service |
| NRL | Naval Research Laboratory |
| NRSM | Nested Regional Spectral Model |
| NWP | Numerical Weather Prediction |
| NWS | National Weather Service |
| PSU | Pennsylvania State University |
| PV | Potential Vorticity |
| PXE | Preboot Execution Environment |

| | |
|---|---|
| QG | Quasi-Geostrophic |
| RAID | Redundant Array of Inexpensive Disks |
| RFC | River Forecast Center |
| RMS | Root Mean Square |
| SMAC | Simplified Method for Atmospheric Correction |
| SNMP | Simple Network Management Protocol |
| SSM/I | Special Sensor Microwave Imager |
| STATSGO | State Soil Geographic Database |
| STATSGO | State Soil Geographic Database |
| TPC | Tropical Prediction Center |
| TRMM | Tropical Rainfall Measuring Mission |
| UKMET | United Kingdom Meteorological Office |
| USDA | United State Department of Agriculture |
| USDA | United States Department of Agriculture |
| USGS | United States Geological Survey |
| UTC | Universal Time Coordinates |
| VGT | Vegetation |
| VIC | Variable Infiltration Capacity |

## LIST OF SYMBOLS

| Symbols | | Description |
|---|---|---|
| % | - | Per cent |
| cm | - | Centimetre |
| cm/hr | - | Centimetre per hour |
| cumec | - | Cubic metre per second |
| $^{O}C$ | - | Degree Celsius |
| g | - | gram |
| hr | - | hour |
| ha | - | Hectare |
| km | - | Kilometre |
| m | - | meter |
| mm | - | Millimetre |
| min | - | Minute |

# CHAPTER I

# INTRODUCTION

A landscape evolving in its land cover and use with a variable and changing climate to produce its hydrologic regime is one of the most salient contemporary issues in the face of Global Change. A particularly sensitive region is Southeast Asia of which India is of primary concern where rapid population growth and socio-economic development over the past several decades has been accompanied by extensive deforestation, expansion of agriculture and irrigation, and stream flow regulation. Consequently most of its water resources have become vulnerable to altered seasonal stream flows, sediment load, and changes in water quality.

Resolution of these irregularities calls for the proper management of surface and ground water resources. Therefore for the adequate implementation of management strategies concerning the land surface hydrology are increasingly being taken into account.

For last decade, remote sensing (RS) has been used in the management of hydrology and water resources, which shows the superiority of RS in impersonality, grandiosity, dynamic and economy as one of the important space information collecting technologies. The modern remote sensing is centered on satellite systems and most of its collaborative research emphasizes the use of satellite data. The large amount of spatially detailed information derived from remote sensing, ground surveys (e.g. digital maps, digital terrain models) or interpolation of point

measurements and handled within a geographic information system (GIS), offers new opportunities for hydrologic modeling.

Hydrological models are simplified representations of actual hydrologic system that allow us to study the functioning of watershed in response to various inputs, and thereby gain a better understanding of hydrological events.

Computer simulation models are a composite of mathematical, empirical and theoretical relationships, which is largely based on system approach to simulation. Now a days hydrologist use it favorably because of its pragmatic advantages. Primary reasons are savings of time and costs and flexibility of modeling as an analytical tool. Particularly in hydrological applications, the computer simulation techniques are available in variety of scales and spatial resolutions. However, there is considerable variation in informational needs and data availability from one area to the next. A framework has been introduced, in which individual hydrological processes (inception, infiltration, surface runoff etc.) and natural resource components are represented by modules that can be linked together to meet specific simulation techniques. This makes updating and replacement of the modules without disrupting other simulators in the modular frame work.

Based on the nature of data representation on a computer simulation model, it has been categorized as *the lumped and distributed* model. A *lumped* model consider a watershed or land units within the watershed as an individual unit, and therefore simulation within the watershed will likely to use an average value for the watershed (or an average value for each land unit within the watershed ). In other words, lumped modes as the models that takes no account of spatial variabilities in the processes, input, boundary conditions, or hydrological properties of watersheds. Conversely, the processes simulated in a *distributed* model are calculated from point to point by using a distribution function or a spatially derived algorithm.

Since the *lumped* model framework is the mere simplification and the *distributed* framework needs huge data. *Quasi-distributed* model came in picture which simplifies the modeling process by subdividing the area into smaller unit with analogous hydrological properties and further could be defined by lumped parameters. Variable Infiltration Capacity (VIC) model is one of such quasi-distributed model.

Based on the evidences of field experiments and remote sensing analyses that spatial variability of precipitation, vegetation covers, topography, and soil heterogeneities play important role in soil moisture distribution, runoff production,

and evaporation, a hydrologic based Variable Infiltration Capacity (VIC) land surface model was developed by Xu Liang at the University of Washington.

The macro scale model is a *quasi-distributed* grid based hydrological model that parameterizes the dominant hydro-metrological processes by considering sub grid spatial variability of precipitation, infiltration and a mosaic representation of vegetation cover. It's a kind of land surface model (LSM) which addresses interactions between the land surface, atmosphere and underlying surface.

Modeling of land surface processes in the context of coupled land-atmosphere prediction has advanced over the last decade with the development of many sophisticated models that represent a concentration of effort by researchers from disciplines such as hydrology, climate modeling and ecology. The transition from numerical climate models to land surface hydrology is widely recognized.

Historically the land surface hydrology is represented by the bucket models, which treat the domain within the grid as homogeneous, and do not allow surface runoff to be generated except when the soil is saturated. The limitations of the bucket models and the advances in plant meteorology and micrometeorology have led to the development of Soil-Vegetation-Atmosphere Transfer Schemes (SVATS). However, these latter approaches also rely on small scale micrometeorological studies and are limited to short time horizons.

The improved representation of the terrestrial hydrologic parameterization at large continental scale became possible with the advent of *Macro scale Hydrological Models* (MHMs), which attempts to represent physical hydrological processes,

having the interactions between biota, soil and water resources over large spatial scales.

However, most of the MHMs are the hybrids of conceptual and physical based components making the parameter estimation more difficult. Conversely, the (VIC) model possesses a physically based component to represent the exchanges of sensible and latent heat with the atmosphere but uses empirical approximations to simulate precipitation-runoff processes and infiltration.

When the model is implemented over a grid mesh, evaporation, energy fluxes, runoff, and baseflow are predicted independently for each grid cell. The fast runoff is represented by direct runoff while the slow component is represented by nonlinear subsurface runoff. Stream flow is then predicted at a specified location by routing runoff and base flow from each grid cell. The VIC model has run at a number of resolutions in global and large basin scales.

Based on the number of layers the model has been categorized as VIC-2L and VIC-3L. The VIC-2L accounts for the two layers of the soil, while the later VIC-3L does for three layers to simulate evaporation, energy fluxes, runoff, and baseflow. The VIC-2L model, includes two different time scales (i.e. fast and slow) for runoff to capture the dynamics of runoff generation. The upper soil layer of the model is designed to represent the dynamic response of the soil to rainfall events, and the lower layer is used to characterize the seasonal soil moisture behaviour.

To better represent the quick bare soil evaporation following small summer rainfall events, a thin soil layer is included in VIC-2L and it becomes VIC-3L. Also, soil moisture diffusion processes between the three soil layers are considered in VIC-

3L.Liang & Xie (2001) developed a new parameterization to represent the infiltration excess runoff mechanism in VIC-3L and combined it effectively with the original representation of saturation excess runoff mechanism.

The desired input data for VIC model includes *Parameter data* and *Forcing data*. *The Parameter data* the significant land surface parameters associated with soil land cover and topography. On the other hand, the *Forcing data* are the atmospheric inputs to the model, including precipitation and temperature.

The intent of my present work is soil and vegetation data base generation for the VIC-2L at the continental scale using numerous global datasets. These input data sets define the view of the landscapes captured by the VIC model, and are important determinants of the model's hydrologic predictions; runoff generation .and to rout runoff into discharge at grid points where gauging stations are located. The specific objective of the study includes:

1. Collection of public domain geo-spatial data on elevation, land use/cover and soil.
2. Generation of soil and vegetation parameters.
3. Converting each of the data set into the file format required for VIC Model.

# 1 CHAPTER II

# 2 REVIEW OF LITERATURE

**This chapter deals with the review of literature on major fields related to this study, which include remote sensing and GIS applications in hydrology, data extractions for DEM/DTM, ground water interaction and classification of hydrological models. It also includes review of work related the Variable Infiltration Capacity (VIC) model and its applications.**

## 2.0 Application of Remote Sensing and GIS

Agrawal *et al*. (2003) used multitemporal SPOT-VGT data for vegetation mapping in south central Asia. The basis of classification is temporal dynamics, *i.e*. the pattern of change of Normalized Difference Vegetation Index (NDVI) values through a temporal domain which reflects the phenology of vegetation, crop cycle and the cropping system of agricultural practices. The temporal profile of NDVI facilitates the discrimination between different vegetation types and different types of cropping pattern.

2.1 Barnsley *et al.* (2000) estimated the land surface albedo and the vegetation biophysical parameter using SPOT-4 VGT and semi-empirical BRDF models for East Anglia (UK), Bordeaux (France) and SE Spain. The data had been collected from the VGT sensor for the period 17th of May to1st of October 1999, covering Western Europe which were atmospherically corrected in-house using the Simplified Method for Atmospheric Correction

(SMAC) and cloud masked using the reflectance information in the blue channel.

Chang *et al.* (2000) explored the possibility of inferring soil physical properties from a multitemporal remotely sensed brightness temperature and soil moisture maps by constructed two artificial neural network models based on physical linkages among space-time distribution of brightness temperature, soil moisture, and soil media properties. Sequence of remotely data from Washita ’92 experiment shows the possibility to infer soil texture from multitemporal brightness temperature and soil moisture data.

Boegha and Thomsen *et al.* (2000) used a new method for a composite evaluation of atmospheric resistance, surface resistance, and evapotranspiration rate. The variables surface temperature (Ts), net radiation (Rn), soil heat flux (G), air temperature (Ta), and calculated on the basis of Landsat-5 TM, which leaves solar irradiance (for computing *Rn*), *Ta*, and air humidity (ea) as the only field data required.

Khan *et al.* (2001) studied an integral part of Guhiya basin for watershed prioritization using remote sensing and geographical information system. 68 watersheds were assessed on the basis of their erosivity and sediment-yield index values using the terrain information derived from geocoded satellite data and 1:50,000 topographic maps. On the basis of sediment yield index values the watersheds were grouped into very high, high, moderate and low priorities.

**2.1 Remote Sensing in Hydrology**

Recent technological innovations in remote and direct acquisition of good data offer unique opportunities for hydrologic and water quality modeling, good data permits the development of accurate models, generation or testing of new hypotheses and extension of models to other areas with limited information.

Rango (1994) presented a detailed description of the theory and application of the remote sensing technology in hydrology and water resources. Chakraborti (1993) in his review paper explained the procedure for watershed resource database creation through remote sensing and their use in runoff and sediment yield models for watershed conservation planning, environmental impact assessment and scenario development.

The conventional methods for land use/cover classification are accurate but expensive, time consuming, difficult to update and repetitive. Now, however, computer and satellite technologies have given us the opportunity to merge data sets and to update the land use/cover information by a low cost operation. Glover, (1984) reported that the cost of conventional data gathering methods for a similar basin is 11 times more than LANDSAT data. Supervised classification of SPOT MS data provides the most cost-effective means of deriving land use/cover classes for evaluation of watershed (Jakubauskas *et al.*, 1992). The current satellite technology has improved the spatial resolution, which is the key to many future detailed land use/cover studies.

Various input parameters of hydrologic models can be derived from remote sensing imageries. Many researchers used land use/cover information derived from satellite imageries and integrated them with GIS for runoff, infiltration, evaporation,

erosion and sedimentation studies. (Young *et al.*, 1987; Johnson, 1989; Jakubauskas *et al.*, 1992; Kouwen *et al.*, 1993; Ross and Tara, 1993). Model of soil loss and runoff developed by the soil conservation service (SCS) including the USLE have also been implemented with input derived from remotely sensed data (Pelletier, 1985).

Since there are many different sources of information on land use/cover, a standardized system of classification has been developed that is compatible with remotely sensed data (Johnsson, 1994). Lillesand and Kiefer (1994) described the mathematical and statistical approaches for the classification scheme. They reported that the algorithm, which is used to maximum likelihood or Gaussian distribution approaches quantitatively, evaluates both the variance and correlation of the category spectral response patterns when classifying an unknown pixel.

## 2.2 Application of GIS in Hydrology

### 2.2.1 Use of GIS

For about a decade, the concepts of data management offered by GIS have heralded a new era for hydrologic and water quality modeling (Singh, 1995). The GIS technology allows modeler to acquire, organize, analyze and display model input and output data (Burrough, 1986). The flexible design of GIS provides the tools to analyze large-scale hydrologic processes and to evaluate the impact of changes in land management on water quality (Burrough, 1989; Rochester *et al.*, 1996).

### 2.2.2 Integration of GIS and Remote Sensing in Hydrologic Modeling

Spatially distributed models of watershed hydrological processes have been developed to incorporate the spatial patterns of terrain, soils, and vegetation as estimated with the use of remote sensing and geographic information systems (GIS) (Band *et al*., 1991; 1993; Famiglietti and Wood, 1991; 1994; Moore and Grayson, 1991; Moore *et al*., 1993; Wigmosta *et al*., 1994; Star *et al*., 1997). This approach makes use of various algorithms to extract and represent watershed structure from digital elevation data. Land surfaces attributes are mapped into the watershed structure as estimated directly from remote sensing imagery (*e.g.* canopy leaf area index), digital terrain data (slope, aspect, contributing drainage area) or from digitized soil maps, such as soil texture or hydraulic conductivity assigned by soil series.

Considerable progresses have been made in coupling GIS with hydrologic and water quality models on the basis of either the loose or close coupling strategy. Vieux (1991) discussed the loose coupling of a distributed hydrologic model with ARC/INFO GIS to evaluate overland flow and nonpoint source pollution in agricultural watersheds. Tim and Jolly (1994) describe the close coupling of the AGNPS model (Young *et al.*, 1989) with the ARC/INFO GIS to evaluate nonpoint source pollution of watershed.

**2.2.3 Data extraction from DEM/DTM**

De Vantier and Feldman (1993) reviewed and discussed various approaches including lumped parameter, physically based and hybrid to hydrologic modeling with respect to their geographic data inputs. They summarized past efforts and current trends in using Digital Terrain Models (DTM) and GIS to perform hydrologic

analyses. The DTM or DEM (Digital Elevation Model) has proven to be a useful and consistent tool for deriving information about the morphology of the land surface.

Many researchers used various GIS technique and DEM/DTM to extract data for hydrological and water quality models (Olivieri, 1991; Opena, 1992; Warwick and Haness, 1994; Smith and Vidmar, 1994; Greene and Cruise, 1995; Garg, 1996; Wang and Hjelmfelt, 1998). They generated a DEM after calculating and interpolating the elevations on a regular grid and concluded that the elevation accuracy depends on spatial resolution.

DEMs. Brown and Bara (1994) used semivariograms and fractal dimensions to confirm the presence and structure of systematic errors in DEMs and suggested filtering as a means to reduce the error. Theobald (1989) reviewed the sources of DEMs and its data structure to identify how bias and errors are produced in DEM generation.

Polidori *et al*. (1991) used fractal techniques to identify interpolation artifacts in a 40-meter DEM created from a 1:25,000 scale map; they suggest that the fractal dimension can be used as a DEM quality indicator by revealing directional tendency or excessive smoothing in the DEM.

Lopez (1997) developed a Topographic data came from the HYDRO 1K digital elevation data set with a ground resolution of 1 kilometer.

### 2.2.4 Ground and Surface Water Interaction

Groundwater–surface water interaction is another important aspect in land–atmosphere interaction studies. Water table positions close to the surface would likely

result in saturation excess runoff, yield evaporation at the atmosphere-demanded rate, and produce a net discharge of groundwater. On the other hand, deep water tables generally indicate drier areas where evaporation is limited by the available soil moisture. In this situation, surface runoff is likely to be generated by infiltration excess runoff mechanism, and groundwater is recharged when infiltration is enhanced. Under both conditions of the water tables, the soil moisture is modified through the groundwater and surface water interactions. Field observations showed that the interactions between surface water and groundwater could alter hydrological consequences, such as runoff production (Waddington et al., 1993), water table fluctuations, and surface hydrology (Verry and Boelter, 1978; Taylor and Pierson, 1985; Whiteley and Irwin, 1986; Devito and Dillon,1993; Devito *et al*., 1996; Katz *et al.,* 1997). Salvucci and Entekhabi (1995) presented a statistical approach to estimate the groundwater table under a steady-state equilibrium condition at the hillslope scale, where the groundwater table is estimated by coupling saturated and unsaturated flows throughout rectangular hillslope domains. Their study showed the importance of interactions between groundwater and surface water (at the steady-state equilibrium condition) to long-term evaporation, surface runoff generation, and groundwater recharge at the hillslope scale.

Levine and Salvucci (1999) used a modified version of MODFLOW to study the interactions between saturated and unsaturated zones under equilibrium conditions for a Canadian catchment of 16 $km^2$ with prairie cover. The groundwater table was estimated through a look-up table-type of iteration approach. Depth to the

water table ranging from zero to the deep drainage asymptote (at 1-cm intervals) is obtained by solving a modified surface water balance model offline (Salvucci and Entekhabi, 1995). The water balance for each depth is stored in a look-up table that is used as input to the MODFLOW. Their study showed that the position of groundwater table would impact the partitioning of rainfall, and that the uncoupled vadose zone models (e.g., SVAT models) would overpredict recharge at the expense of evaporation when the groundwater table is deep. The concept and hydrologic characteristics of the TOP model, which considers the effects of topography and groundwater table on water and energy budgets, have been implemented in some land surface models (Famiglietti and Wood, 1994; Peters-Lidard *et al.,* 1997; Chen and Kumar, 2001; Ducharne *et al*., 2000; Koster *et al.,* 2000). However, the inclusion of the groundwater table is again under a steady-state assumption. Walko *et al.* (2000) implemented a modified form of the TOP model into the Land Ecosystem–Atmosphere Feedback (LEAF-2) model. Recognizing the limitation of the steady-state assumption, they modified the steady-state expression of the local height of water table in the original TOP model.

### 2.3 Concepts and Classification of Models

Crawford *et.al* (1966) described Hydrological model as an interface between data and decision making that use watersheds as the fundamental spatial unit to describe the various components of the hydrologic cycle.

Hydrological model provides quantitative expression of the observation, analysis, and prediction of the time variant interaction of various hydrological processes for use in planning, design, and management/operation of hydrologically related structures. (Fleming, 1975; Schulze, 1987)

With rapid developments in computer technology and hydrology, the application of computer based hydrological models can only continue to increase in the near future. A hydrological system is represented as a model and its behaviour is studied by simulation. Digital simulation is desirable in watershed research because it is a complex system to be analysed by mathematical techniques. In digital simulation, systems model is developed from a number of mathematical expressions that represent various processes of the system and the simulation is carried out using a computer. (Seth, 2000)

Generally, a model can be defined as a deliberately simplified construct of nature erected for the purpose of understanding a phenomenon (Batchelor, 1994). A watershed hydrology model is an assemblage of component models corresponding to different components of the hydrologic cycle (Singh, 1995).

Most quantitative hydrologic models can be classified as deterministic, parametric, stochastic or a combination of these. A completely deterministic model would be one arrived at through consideration of the underlying physical relationships and would require no experimental data for its application. A parametric model may be thought of as deterministic in the sense that once model parameters are

determined, the model always produces the same output from a given input. On the other hand a parametric model is stochastic in sense that the parameters depend on the observed data and will change as the observed data changes. A stochastic model is one whose outputs are predictable only in a statistical sense (Haan, 1977).

The models are also classified as lumped and distributed models. A lumped model represents the physical system as spatially homogeneous units and neglects the spatial variability of the input with the system. Distributed models on the other hand, assume that the physical system is made of uniform and discrete sub units, each characterized by a homogeneous set of input parameters (Chow *et al.*, 1988).

The spatial scale can be used as criteria to classify models into small watershed (less than 100 $km^2$), medium-size watershed (100 to 1000 $km^2$) and large sized watershed (greater than 1000 $km^2$) models (Singh, 1995). Based on land use, the watershed may be classified (Singh, 1994) as agricultural, urban, coastal, forest, desert, mountainous, wetland and mixed land. The hydrologic processes are different in their evolution in these different watersheds and hence their models are clearly different.

As a result most models have combined aspects of both approaches and subdivide the watershed into smaller elements with similar hydrologic properties that can be described by lumped parameters. This model type is commonly referred to as partially distributed, or quasi-distributed. Commonly used physically based distributed hydrological models require gridded information in order to effectively

represent the impacts of the spatial distributions of meteorological, hydrological, and topographical data, and soil type and land cover characteristics. (Guo *et.al*, 2004) Variable infiltration capacity (VIC) model is one such hydrological model.

## 2.4 Variable Infiltration Capacity (VIC) Model

Boer et al. (2000) evaluated the use of generated daily climatic data from the monthly means in simulation studies to overcome the problem of data scarcity. Two simulation models, APSIM and VIC were run using the generated and observed daily climatic data. It was found that the outputs from the models resulted from the generated and observed daily climatic data were not significantly different. This result promotes the use historical monthly climatic data to assess historical response of biological systems to variable climate.

The VIC (Variable Infiltration Capacity) model as a macroscale hydrologic model uses the concept of subgrid variability of infiltration capacity and allows different vegetation types within each grid cell (Wood *et al*. 1992, Liang *et al.* 1994, Liang *et al.* 1996, Nijssen *et al.* 1997, Cherkauer & Lettenmaier 1999). The model was designed to represent surface energy and hydrological fluxes and states at scales from large river basins to the entire globe, using an aerodynamic representation of the latent and sensible heat fluxes at the land surface. When the model is implemented over a grid mesh, evaporation, energy fluxes, runoff, and baseflow are predicted independently for each grid cell. The fast runoff is represented by direct runoff while the slow component is represented by nonlinear subsurface runoff. Streamflow is then

predicted at a specified location by routing runoff and baseflow from each grid cell. The VIC model has run at a number of resolutions in global and large basin scales.

The spatial probability distribution model, in its one-layer form, has been used to model the land surface in GCMs by Dumenil and Todini (1992). The two-layer version of the model incorporates a nonlinear drainage (base flow) representation, and an explicit energy-driven Penman-Monteith representation of vegetation. Multiple land cover types, including bare soil, are modeled using a "tile" approach (aggregates all occurrences of a given land cover type within the area to a single equivalent sub area). Data base creation for soil vegetation and meteorological parameters should be done.

The Variable Infiltration Capacity VIC-2L model developed by Liang *et al.*(Liang et al 1994), includes two different time scales (i.e. fast and slow) for runoff to capture the dynamics of runoff generation. The upper soil layer of the model is designed to represent the dynamic response of the soil to rainfall events, and the lower layer is used to characterize the seasonal soil moisture behaviour.

Abdulla et al. (1995) and Lettenmaier (1995a; b) have developed and tested a regional parameter estimation scheme for the VIC-2L model. Using a set of 40 catchments in the Arkansas-Red River basin with drainage areas in the range 100 to 10,000 km 2 for which historical stream flow and meteorological records exist, the parameters of the VIC-2L model were estimated using a search procedure. Regional regression equations were then developed to relate the estimated VIC-2L parameters

for the gauged catchments to catchments characteristics derivable from digital elevation, soils, climatalogical, and land cover data. The prediction equations were tested using observed stream flow data for test catchments not in the training data set, and to predict streamflow hydrographs for the entire Arkansas-Red River system.

To better represent quick bare soil evaporation following small summer rainfall events, a thin soil layer was included in VIC-2L (Liang *et al.*, 1996), and VIC-2L became VIC-3L.

Nijssen et al. (1997) coupled the VIC model with a simple grid-based network routing scheme (including both within grid cell routing and channel routing) to study streamflow simulations for continental- scale river basins. They found that the integrated model (i.e., VIC plus the network routing scheme) performs quite well over moist areas in their study. For arid and semiarid areas, however, their studies indicated difficulties in reproducing monthly observed streamflows

Sridhar *et al.* evaluated the performance of the VIC model using surface energy budget measurements through the Oklahoma Atmospheric Surface-layer Instrumentation System (OASIS) project measurements for the period of June 1999 through May 2000. The modeled net radiation and latent, sensible and ground heat fluxes were compared with the observations for model evaluation.

Nijssen et *al* (2001) made Global Retrospective Estimation of Soil Moisture for year (1980-93). The Variable Infiltration Capacity (VIC) land surface model was used to produce a set of derived fluxes and state variables, including snow water

equivalent, evapotranspiration, runoff, and soil moisture storage. Comparison with observations and existing climatology shows that (1) the interannual variation in simulated snow cover extent is similar to observations in Eurasia but underpredicted in North America; (2) the components of the global and continental water balance are similar to those in previously produced climatologies, although runoff is somewhat lower; (3) patterns of simulated soil moisture storage are similar to the climatology of Mintz and Serafini, but the more sophisticated VIC hydrological model produces a larger range in soil moisture; and (4) the annual cycle and spatial patterns in soil moisture compare well with soil moisture observations in Illinois and in central Eurasia, but mean modeled soil moisture is somewhat lower than observed, and observed soil moisture shows a greater interannual persistence than do the simulations

Nijssen *et al.* (2001) simulated energy and water fluxes over large continental river basins using macroscale hydrological models (MHMs). A methodology for model parameter transfer is described that limits the number of basins requiring direct calibration. The model Parameters initially were estimated for nine large river basins. As a first attempt to transfer parameters, the global land area was grouped by climate zone, and model parameters were transferred within zones. The transferred parameters were then used to simulate the water balance in 17 other continental river basins. On a continental basis, the changes in runoff and evapotranspiration were much larger. A diagnosis of simulation errors for four basins with particularly poor results showed that most of the error was attributable to bias in the Global

Precipitation Climatology Project (GDCP) Precipitation products used to drive the MHM.

Warrach *et al.* (2002) studied Topographically Controlled Runoff Simulation in a Soil-Vegetation–Atmosphere Transfer Model. He used VIC model and a modified TOPMODEL approach to incorporate sub-grid variability in soil moisture and runoff production into soil–vegetation–atmosphere transfer (SVAT) model. The study showed that, during low flow periods, the runoff simulation was superior when using the TOPMODEL-based equations, especially during the rising limb of the autumn hydrograph. A main drawback of the modified VIC-model approach, especially for regional and global application, was that, with five free parameters, considerably more model calibration is required. TOPMODEL, on the other hand, requires only the determination of one free parameter. However, a TOPMODEL approach does require extensive preprocessing of topographic data, and issues concerning resolution of the data used become relevant.

Suoquan *et al*. (2002) simulated terrestrial hydrological processes for the entire Yangtze river basin using VIC-3L land surface model, which was applied to the Baohe River basin. The water fluxes of the Baohe river basin are simulated using the VIC-3L model at a spatial resolution of approximately 4 km. The model was run at a daily time step. Differences in model-simulated water fluxes resulting from using the two different data sources (i.e., MODIS versus REDC) on information of land cover classification and Leaf Area Index (LAI) were compared. Model-simulated daily runoff was routed through the Baohe River basin network and compared with

the daily observed streamflow measured at Jiangkou hydrological station at the outlet of the Baohe River basin from 1992 to 2001. This study indicates clearly the important role that remote sensing (e.g., MODIS data) plays in improving model simulations.

Xie *et al*. (2004) applied the VIC-3L model coupled with a routing scheme for the Yellow river basin. The input data including soil data from NOAA hydrology office, vegetation data from LDAS information and the available forcing data for the period 1980–1990 were compiled with a 50 km grid resolution. The model was applied to the basin and the simulated daily runoff is routed to the outlet of two stations and compared to monthly observed streamflow at these stations. Results showed that the model can simulate the observations accurately.

Liang and Xie (2001) extended the current version of the widely used VIC-3L model with a statistical approach to include the infiltration excess runoff generation mechanism by considering effects of subgrid spatial heterogeneity of soil properties. The current version of the VIC-3L model already incorporates saturation excess (Dunne) runoff generation through a probability distribution function of soil storage capacity. The new statistical approach is consistent with the treatment of the VIC in its original form for the saturation excess runoff calculation.

Xu Liang (2003) made the evaluation of the effects of surface water and groundwater interactions on regional climate and local water resources. In this project, the impact of surface and groundwater interactions on soil moisture,

evapotranspiration, runoff, and recharge are investigated. Through the two year project a new parameterization to represent surface and groundwater interaction dynamics for land surface models is developed and implemented into a the VIC-3L) is applied to a watershed in Pennsylvania over multiple years. Results show that VIC can properly simulate the movement of the daily groundwater table over multiple years at the study site.

### 2.4.1 VIC model in PILP Project

The hydrological based Variable Infiltration Capacity (VIC) land surface model has actively participated in various phases of the Project for Intercomparison of Land-surface Parameterization Schemes (PILPS) (Shao and Henderson-Sellers, 1996; Chen *et al.*, 1997; Liang *et al*., 1998; Lohmann *et al*., 1998; Wood et al., 1998; Pitman *et al*., 1999) since the beginning of the PILPS project.

Based on the various PILPS activities and different applications of the VIC model at various basins ranging from small watersheds to continental and global scales (Wood *et al.,* 1997) under different climate conditions, the VIC model has been constantly improved over the past years. At the beginning, the version of the two-layer VIC model (i.e., VIC-2L) participated in phase-1 (1a, 1b, and 1c) and phase-2b of the PILPS. The VIC-2L model is a semidistributed grid-based hydrologic model that parameterizes the dominant hydrometeoro- logical processes by considering subgrid spatial variabilities of precipitation and infiltration, and a mosaic representation of vegetation cover (i.e., different vegetation covers and bare soil). The

model uses two soil layers and one vegetation layer with energy and moisture fluxes exchanged between the layers. The upper soil layer is designed to represent dynamic response of soil moisture to rainfall events, and the lower layer is used to characterize seasonal soil moisture behavior. Two different time scales of runoff (fast runoff and slow runoff) are included in the model to capture the dynamics of runoff generation. The fast component of runoff is represented by surface runoff, and the slow component is represented nonlinearly by subsurface runoff. Based on the HAPEX study of the PILPS (phase-2b), VIC-2L was modified to add one thin surface layer (i.e., three-layer variable infiltration capacity (VIC-3L)) to better represent bare soil evaporation process after small summer rainfall events. In addition, diffusion process was included in the representation of the VIC soil column. This version of the VIC-3L model was used in phase-2a of the PILPS study.

In the phase-2c study, the version of the VIC model with a better ground heat flux parameterization (Liang *et al.,* 1999) was used that resulted in more reasonable ground heat flux simulation (Liang *et al.,* 1998) among other features of the VIC model.

In the PILPS phase-2e, the version of the VIC with better features of frozen soil processes for cold climate conditions (Cherkauer and Lettenmaier, 1999) was used. The VIC model did not participate in the PILPS phase- 2d.

It is clear that over the course of various phases of the PILPS and other applications, the VIC has been constantly improving. Since the PILPS phase-2e, two

more major improvements with the VIC model have been implemented. One of them is the ability of VIC to generate both infiltration and saturation excess runoff within a model computational grid cell simultaneously to improve the partitioning of water and energy budgets under a wide range of wet and dry climate conditions. The new parameterization of infiltration and saturation excess runoff considers effects of subgrid-scale spatial variability of soil properties.

In the phase-2c of the PILPS inter comparison study, Lohmann *et al.* (1998) showed that a number of land surface schemes have too much runoff in the summer due to their wet soil moisture, while others have too little runoff most of the time. That study suggested that infiltration excess runoff process under dry conditions should be improved.

## 2.1.1.1.1 CHAPTER III

# MATERIALS AND METHODS

The chapter presents the scientific rationale and the detail procedures involved in soil and vegetation data sets generation for VIC-2L model. Initially the model overview and description has been made. The methodology in the study is hub around the generation of soil, land use/land cover and DEM data at common projection i.e. Albers conical equal area projection and uniform resolution i.e.10 km resolution. The acquisition and extraction of public domain global data sets have been explained for generating soil and DEM maps generation. The commonalities of transformation from the 45 class land use/cover data to 12 class UMD classification scheme are explained. During the image processing and GIS analysis, the different programs of the remote sensing and GIS software are characterized with their limitations. The chapter saliently describes the derivation of the different soil and vegetation parameters required for the VIC-2L model and finally, it also explains the exhaustive steps for linking the generated parameters with the generated maps, by raster attribute map generation followed by *ASCII* format.

### 3.1 The Study Area

The database has been primarily generated for India, however it also covers some part of it's subcontinent including Andaman & Nicobar and Lakshwadeep islands of Indian Ocean region. The geographic extent of the region is from 65.51° to 100.65°E longitude to 2.45° to 37.45°N latitude and covers an area of 12187500 $km^2$. The geographical location of the region is physically dominated by the monsoon

system. Generally there are four climatic seasons, *summer, winter, mansoon(rainy) and spring*. The region is having diversified relief with annual rainfall varying from 100 mm in desert area to 11000 mm in northeastern hills. This high degree of spatial and temporal variability in rainfall has led to a variety of climatic zones ranging from arid to moist tropical rainforest, and occurrence of devastating droughts and floods. The mean temperature varies from 2° to 50°C defining the landmasses into different zones viz., temperate and alpine.

The region has a complex variety of physiographic patterns, with extensive mountain ranges, large river basins, platues and long coastal line bordered by Arabian Sea, Bay of Bengal and Indian Oceans

**3.2 Hardware and the software used**

The research work was carried out in the Water Resource Division of *IIRS*, Dehradun; facilitated with *Compaq* Workstation having *Pentium III* processor of *733 MHz, 256 MB RAM* and 50GB of hard disc space. The system is installed with softwares like *ILWIS 3.2, ERDAS8.6, ArcMap3.2, ENVI 4.1* and *Micro Soft*. The data visualization, image processing and GIS analysis were carried out using the remote sensing and GIS softwares. The Excel package of *Microsoft Office 2000* was used to analyse the data for requisite calculations.

The *3dem* software was used to generate the DEM. This was downloaded from the website http://www.visualizationsoftware.com/3dem. It is a product of Visualization Software LLC by Richard Horne and produces 3-dimensional terrain scenes by flyby animations from a wide variety of freely available data sources

including *USGS Global 30 Arc Second Elevation Data Set*, the data used for the DEM generation in the project.

### 3.3 Data Acquisition

The data acquisition had been made using the global data and the information derived from the global data sets. Global data used for the research work includes the *MM5 V3 Terrain* files for soil map generation and *GTOPO30*, Global 30 Arc Second Elevation Data for DEM generation. The land use/cover map was prepared using the available land use/cover data for central south Asia (propriety of *IIRS*) based on *SPOT-VEGETATION* data. Apart from these, the complex parameter requirement of the VIC model was either made from the numerous research work or values derived from the satellite data.

#### 3.3.1 USGS GTOPO30 elevation data

For generation of DEM, GTOPO 30 data was used in the study, which had been downloaded from the website *http://edcdaac.usgs.gov/gtopo30* of *LP DAAC User Service*. The data is a global digital elevation model *i.e.* the extent of latitude from 90˚ S to 90˚ N and the full extent of longitude from 180˚ S to 180˚ N. The horizontal grid spacing of the data is 30 *arc seconds* (approximately 1 kilometer). The elevation values range from -407 to 8,752 meters. In the DEM, ocean areas have been masked as "no data. Lowland coastal areas have an elevation of at least 1 meter.

For easier distribution, the data is divided into 27 tiles shown in Plate (3.1). The two tiles E100N40 and E060N40 shown in Plate (3.2) covering the region were used for derivation of DEM.

#### 3.3.2 MM5 V3 terrain data

The source data for generating the soil texture data has been obtained from the *MM5 V3 Terrain* file. It is a having multi-band (17) soil texture data at varying resolution from 1 degree to 5 minutes, for the corresponding two layer depth of soil profile viz.0-30cm depth and 30-100cm depth. The soil data files are based on *FAO* and *STATSGO* data freely provided and supported by the Mesoscale

available at *ftp://ftp.ucar.edu/mesouser/MM5V3/TERRAIN_DATA/* .

**3.3.3 Land use/land cover data of south central Asia**

Land use/land cover map of south central Asia, propriety of Indian Institute of Remote Sensing (IIRS) and further is part of the on-going global land cover-mapping project (GLC 2000); was used for the vegetation input generation of the VIC model. The virtue of the data is its consistency and uniformity with 1x1 km grid resolution over the entire south central Asia. The vegetation mapping of the data is based on the multi temporal *SPOT VEGETATION* data. The data is classified in 45 land use/land cover classes. An unsupervised clustering algorithm (ISOCLASS) on the nine-month the maximum *NDVI* composite *(MVC)* images spanning from November 1999 to December 2000, was used to define classes within the vegetated and non-vegetated stratum. The *FAO* land cover classification scheme was adopted for defining the classes. The urban area mapping of the data relies on Defense Mapping Meteorological Satellite Program (DMSP) 10.

**3.3.4 LDAS information**

Land Data Assimilation System *(LDAS)* available at; *http://ldas.gsfc.nasa.gov* is a model control and input / output system (consisting of a number of subroutines, modules written in Fortran 90 source code) that drives multiple online one

dimensional land surface models (LSMs) to simulate sub-grid scale variability. It makes use of various satellite and ground based observation systems within a land data assimilation framework to produce optimal output yields of land surface states and fluxes.

Most of the vegetation parameters values for the dataset generation were obtained from LDAS vegetation parameters mapped according to UMD classification Scheme. The parameters under the LDAS scheme were derived by averaging the physical parameter data sets based on other vegetation classification schemes of IGBP, BATS, NCAR LSM, SiB, SiB2 and Mosaic together to form a generic parameter value for UMD vegetation classes

#### 2.1.1.2 3.4 VIC-2L Model Overview

The Variable Infiltration Capacity model-2layer (VIC-2L) is a surface water and energy balance model designed for large-scale applications. It can be applied to grid cells, typically with spatial dimensions from 1/8 to 2˚ degrees latitude by longitude, connected so as to represent large continental river basins.

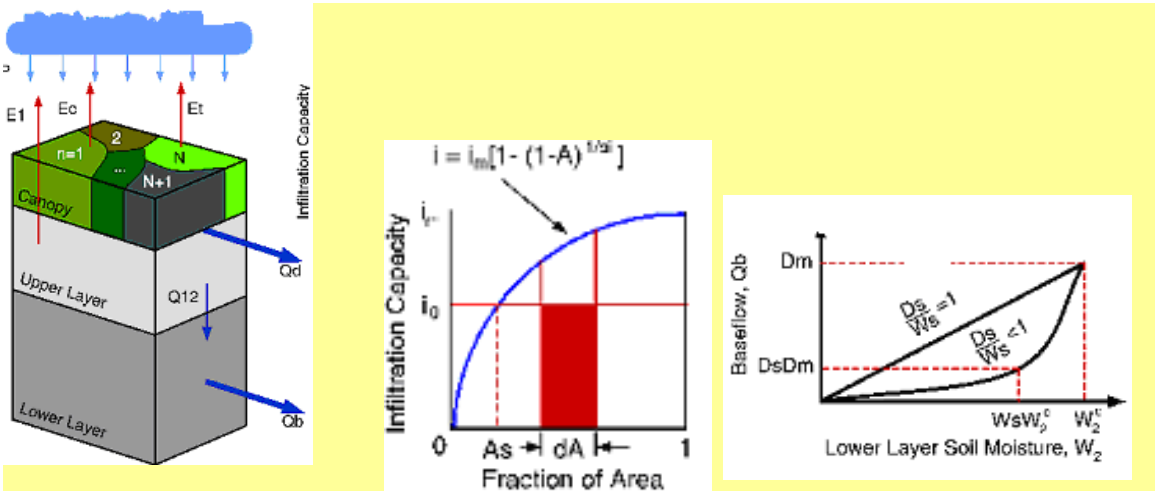


**A. Soil layer** **B. Infiltration curve** **C. Base flow**

**Fig. 3.1: Variable Infiltration Curve-2Layer Model (VIC-2L)**

Features of interest include the eponymous ***variable infiltration curve*** (Liang et al., 1994) as shown in Fig.3.1B of the soil and vegetation column schematic, which scales the maximum infiltration ($i_m$) by a non-linear function of fractional grid cell area to enable runoff calculations for sub grid-scale areas. Using the infiltration formulation, model effectively assumes that runoff is generated by those areas for which precipitation, when added to soil moisture storage at the end of the previous time step, exceeds the storage capacity of the soil *i.e.* there is no canopy storage (through fall = precipitation).

Another feature is the specification of empirically based ***Arno baseflow curve*** (Liang et al., 1994) as shown in Fig.3.1C. It is a function of soil moisture in the lowest soil layer. This relationship is non-linear at high soil moisture contents, producing rapid baseflow response in wet conditions and there by causing subsurface runoff.

Three types of evaporation are considered in the model: evaporation from canopy layer of each vegetation class, transpiration from each of the vegetation classes, and evaporation from bare soil. Evapotranspiration from each vegetation type is calculated using a *Penman-Monteith formulation* (Liang et al. 1994). Total evapotranspiration over a grid cell is computed as the sum of the above components, weighted by the respective surface cover area fractions.

The operational model of the model includes *Water balance mode* and *Energy balance mode*. The *Water balance mode* uses approximations for the relevant energy terms, such as the effective surface temperature as air temperature. It also includes; a) evaporation from canopy and surface layer, transpiration from canopy, b) vertical moisture transport only, in upper two layers either through evapotranspiration, or drainage and c) baseflow, or horizontal transport from bottom layer. The run time step is daily.

Whereas, the *Energy balance mode* calculates all water and energy fluxes near the land surface. The surface energy balance includes; a) Long and short wave radiation fluxes and b) Latent heat, sensible heat and ground heat fluxes. The run time step for the energy balance mode is 1 or 3 hours.

The result of the VIC-2l model gives the output as runoff which is subsequently the input for the routing model. The routing model uses the linear transfer functions with DEM to rout runoff into discharge at grid points where gauging stations are located.

#### 2.1.1.3 3.5 Projection System used for the Datasets

All the data sets in the present research work were prepared in *Albers conical equal area* the *projection.* The projection system is mathematically based on a cone that is conceptually secant on two parallels. It retains its properties at various scales, and individual sheets can be joined along their edges.

This projection possesses the property of equal-area, and the standard parallels are correct in scale and in every direction. The equal-area implies for the area bounded by any pair of parallels and meridians is exactly reproduced between the image of those parallels and meridians in the projected domain *i.e.* the projection preserve the correct area. Thus, there is no angular distortion (*i.e*., meridians intersect parallels at right angles), and conformality exists along the standard parallels. Moreover, like other conics, Albers Conical Equal Area has concentric arcs for parallels and equally spaced radii for meridians. Parallels are not equally spaced, but are farthest apart between the standard parallels and closer together on the north and south edges.

### 2.1.2 3.6 Raster Grid Map Generation

The database generation of the project is at the continental scale, which primarily aims at for all the Indian basins. However, the geo-bounds for the study have been taken in order to include the natural extent of all the basins. As the selected geo-bound is not the specific one, a raster grid map was generated which considers for the same grid resolution and projection as that of generated datasets. Using *ILWIS*

and *ERDAS* the raster grid map was generated, which serves as the base map for making DEM, soil and land use/cover maps.

Initially, a grid map was created in *ILWIS* using the *ID grid operation* which uses a coordinate system to create a *polygon map* (rectangular grid cells with a unique ID). The following specifications are made for the grid map generation:

**Projection system**

| | |
|---|---|
| **Projection:** | **Albers conical equal area** |
| Datum | WGS 84 |
| Spheroid | WGS 84 |
| Central latitude | 20 m |
| Central meridian | 78 m |
| First parallel | 12 m |
| Second parallel | 28 m |
| *2.2 False easting* | *2000000 m* |
| False northing | 2000000 m |

**Origin of the coordinate**,

***continued on next page**

X: 863000 m

Y: 172200 m

**Grid Size (Width, Height),**

Width: 10000m, and

3 Height: 10000m

**No. of vertical, horizontal grids:**

*Vertical grids:* *375, and*

*Horizontal grids:* *325*

The generated out put was exported from ILWIS as "*eoo."* file format , and then imported in ERDAS as "*arc coverage."* format. The vector file was finally rasterized by using *vector to raster* function of *ERDAS.*

**Table 3.1: The corner pixel information of generated raster grid map**

| Corner position of the raster grid map | File Coordinate | Geographic | Albers conic equal area projection |
|---|---|---|---|
| | *Samples(Y)/lines(X)* | *Lat/Long* | *Northing / Easting* |
| Upper left corner | X: 1 | Long: 65˚ 57' 44.48" | Easting: 863000 m |
| | Y: 1 | Lat: 37˚ 20' 5.85" | Northing: 172200 m |
| Upper Right corner | X: 1 | Long: 100˚ 45' 30.54" | Easting: 4113000 m |
| | Y: 375 | Lat: 36˚ 07' 30.25" | Northing: 172200 m |
| Lower left corner | X: 325 | Long: 68˚ 04' 36.2" | Easting: 863000 m |
| | Y: 1 | Lat: 3˚ 06' 43.7" | Northing: 3922000 m |
| Lower right corner | X: 325 | Long: 98˚ 23' 17.82" | Easting: 4113000 m |
| | Y: 375 | Lat: 2˚ 20' 40.07" | Northing: 3922000 m |

The corner pixel information obtained from the raster grid map shown in Table 3.1. The origin coordinate of the grid map is the lower left corner in *metric coordinate system* specified by the X and Y coordinates.

**3.7 Soil Dataset Generation**

The primary phases of soil data set generation in the research work included; soil texture data generation followed by the soil parameter estimation and finally by the raster data generation for each of the parameters.

### 3.7.1 Derivation of Soil texture data at model grid resolution

The source data for generating the soil database has been obtained from the website *ftp://ftp.ucar.edu/mesouser/MM5V3/TERRAIN_DATA/* . The data files in the downloaded directory of *MM5V3/TERRAIN_DATA* include *SOILCAT.TAR.gz* and *SOILCATB.TAR.gz* files. These files signify each of the soil horizons (layers) as the top soil layer (0 - 30 cm) and the bottom soil layer (30 - 100 cm) respectively. Each of the file once unzipped and untarred yielded 4 files indicated in the Table 3.2.

**Table 3.2: The Untarred files of *MM5 V3 Terrain* data**

| The tarred files | The untarred file type at different resolutions | | | |
|---|---|---|---|---|
| | 1 degree | 30-mins. | 10 min | 5 min. |
| SOILCAT.TAR.gz | SOILCAT.60 | SOILCAT.30 | SOILCATB.10 | SOILCAT.05 |
| SOILCATB.TAR.gz | SOILCATB.60 | SOILCATB.30 | SOILCATB.10 | SOILCATB.05 |

Each of the sub files of *SOILCAT.TAR.gz* and *SOILCATB.TAR.gz* at different resolutions. The global data are having 17 bands; each specifies the unique soil texture as indicated in Table 3.3. The 5 minute data files of specified layers *i.e. SOILCAT.05* and *SOILCATB.05* implies for 9.26 km spatial resolution, which seems to be the most appropriate for the requisite data base generation

**Table 3.3: Band information of MM5 V3 Terrain data**

| **Band Number** | **Soil Texture and other** |
|---|---|
| Band 1 | Sand |
| Band2 | Loamy Sand |
| Band3 | Sandy Loam |

| | |
|---|---|
| Band4 | Silt Loam |
| Band5 | Silt |
| Band6 | Loam |
| Band7 | Sandy Clay Loam |
| Band8 | Silty Clay Loam |
| Band9 | Clay Loam |
| Band10 | Sandy Clay |
| Band11 | Silty Clay |
| Band12 | Clay |
| Band13 | Organic Materials |
| Band14 | Water |
| Band15 | Bedrock |
| Band16 | Other |
| Band17 | No data |

However, prior to importing the scientific data sets ENVI image headers were built enabling the data to be viewed in ENVI and subsequently geo-located. The header information primarily includes the number of samples, number of lines, number of bands (17) and interleave type (band interleaved by pixels *i.e.* BIP).As each of the bands show the global coverage, the latitude and longitude follows the range;

$$-90^{\circ} \le \varphi \le 90^{\circ}, \text{ and}$$

$$-180^{\circ} \le \lambda \le 180^{\circ}$$

Moreover, the data content of the files are assumed to be valid at the center of a grid box, which implies that;

For 1-degree data*;*

*Total no of data points = 360 x180.*

And the similar calculative parlance for the 5-minute data*;*

*Total no of data points = (360x12) x (180x12) i.e.*

*Total no of samples =360x12=4320,*

*Total no of lines = 180x12 =2160.*

Therefore the HDF file information for the importing the soil data was;

*ENVI*

*Description = {*

*File Imported into ENVI.}*

*Samples = 4320*

*Lines = 2160*

*Bands = 17*

*Header offset = 0*

*File type = ENVI Standard*

*Data type = 1*

*Interleave = bip*

*Sensor type = Unknown*

*Byte order* = Host (Intel)

Thus, each layer depth data of 5 min. data of dimension *(4320 x 2160 x 17)* in the *BIP* format were imported in *ENVI*.

**3.7.1.1 Subseting the soil data**

The imported data are having the global coverage of file size 158,630,400 bytes. To reduce the data size, a rough subsets corresponding to the geo-bound (60.00°E to 102.00°E longitude to 0.00° to 40.00°N latitude) for each of the bands were made using the resizing program in ENVI. While resizing the data, input image resize factor was kept 1 and type of interpolation as *Pixel Aggregate*

The sample and lines worked out during spatially subseting the data is based on calculation of center of grid box as shown in Table 3.4.

**Table 3.4: Samples and Line values for subseting the soil data**

| **Corner Position** | **Sample Value(Y)** | **Line Value(X)** |
|---|---|---|
| Upper left corner (60°E , 38°N) | 2160+12 x 60 = 2880 | 50 x 12 = 600 |
| Lower right corner (101°E ,2°N) | 2160+12 x 102 = 3372 | 90 x 12 = 1080 |
| Upper Right corner (101°E , 38°N) | 2160+12 x 102 = 3372 | 50 x 12 = 600 |
| Lower left corner (60°E ,2°N) | 2160+12 x 60 = 2880 | 90 x 12 = 1080 |

This implies that the subset data (5 minute grid spacing) is defined for;

*No of samples = 3372 - 2880 = 492*

*No of lines = 1056 - 624 = 432*

*Total no of grid points = 492 x 432 = 212544*

The resized data having resolution of 8 bit gray scale were saved as "*ERADAS 7.5 LAN"* (Direct Read), which has been imported in *ERADAS IMAGINE* as ".img". format.

### 3.7.1.2 Layer stacking of the resized images

The projection system of the entire 17 band imported data is not defined. However, to georeference the data each of its bands need to be georefernced. *Layer stacking* in *ERDAS* enables to stack all the layers so that these could be georefernced by mere georeferencing of any one of its layer.

The program implies for building a new multi-band file from images of various pixel sizes, extents, and projections. It made the input bands resample and re-projected to a common user-selected output projection and pixel size. Each of the resized images having file extension as ".img" were added one by one to make a stack list of the 17 layers for both of soil horizons.

### 3.7.1.3 Geo-Referencing of stacked layers

Geo-referencing refers to the process of assigning map coordinates to image data i.e. the map location for every pixel. The process is associated with the Ground Control Points **(**GCPs), which are specific pixels in an image for which the output map coordinates (or other output coordinates) are known. It consists of two X, Y pairs of coordinates. One is source coordinate and other is the reference coordinate. The source coordinate are the data file coordinates in the image being rectified. And the reference coordinates are the coordinates of the map or reference image to which the source image is being registered. Here, the georeferencing of the imported data has been made at two phase as described below.

**A. Geo-referencing of the layer-stacked images in *Geographic lat/long***

The stacked images had only information about the four corner- pixel values in terms of lines and samples as given in table (3.4), which was implying for the

corresponding lat/long positions. While georeferencing the geometric model was set as Polynomial of the first order transformation as it needed minimum of 3GCPs, conversely to the second order which requires minimum of 6GCPs. The projection system was set at Geographic lat/long with datum and spheroid as WGS 84. The possible way of geo-referencing at this stage was the key *board method*. Using the key *board function* the values of samples and lines were entered as the source coordinate and the corresponding values of lat/long as the reference coordinate, as shown in Table 3.1

Consequently, the procedure made all the layers of the stacked image geo-referenced at geographic lat/long. Using the out put image, the values of samples and lines were worked out for four different lat/long locations referred to the four corners of the *base raster grid map* mentioned in Table 3.1 worked out line and sample values of subset image of the soil data is given in Table 3.5

**Table 3.5: Lines and sample values of subset image corresponding to raster grid map**

| Corner position of raster grid map | Geographic Coordinate in subset image | Corresponding Samples/Lines values in subset image |
|---|---|---|
| ULX | 65˚ 57' 44.48" | X:9 |
| ULY | 37˚ 20' 5.85", | Y:68 |
| URX | 100˚ 45' 30.54" | X:11 |
| URY | 36˚ 07' 30.25" | Y:97 |
| LLX | 68˚ 04' 36.2" | X:413 |
| LLY | 3˚ 06' 43.7" | Y:97 |
| LRX | 98˚ 23' 17.82" | X:428 |
| LRY | 2˚ 20' 40.07" | Y:437 |

**B. Geo-referencing of the layer-stacked images in *Albers conic equal area***

Once the points had been located, the raw (without projection) stacked image was again geo-referenced by referring the raster grid map. While doing geo-referencing the geometric model was set the same, *i.e*. polynomial with first order transformation but the projection system was set at Albers Conical Equal area projection. The worked out values of samples and lines were used as the source coordinate and corner pixel location of raster grid map as the reference coordinate. Table 3.6 shows the GCPs used while georeferencing.

**Table 3.6: GCPs used for georeferencing soil data in Albers conical projection**

| GCPs | Source Coordinate | Reference Coordinate | |
|---|---|---|---|
| 1 | X:9 | Easting: | 863000 m |
| | Y:68 | Northing: | 172200 m |
| 2 | X:11 | Easting: | 4113000 m |
| | Y:97 | Northing: | 172200 m |
| 3 | X:413 | Easting: | 863000 m |
| | Y:97 | Northing: | 3922000 m |
| 4 | X:428 | Easting: | 4113000 m |
| | Y:437 | Northing: | 3922000 m |

Consequently, the layer-stacked images were made geo-referenced at the desired model grid projection.

**3.7.1.4 Resampling of data using nearest neighborhood**

The term resampling implies for creating a new image by forcing a new X-Y grid onto the warped image of the transformed input. After making the transformation the out put image had been resampled.

*In Resampling, Resample Method: Nearest Neighbor*

*Upper Left: X = 172200 m, Y = 3922000 m*

*Lower Right: X = 172200 m, Y = 4113000 m*

*Out Put Grid Size: X =10000 m, Y = 10000 m*

The operation assigned each pixel a new data value from the input image by using *nearest_neighbor* resampling method that uses the value of the closest pixel to assign to the output pixel value. Moreover, by using the resampling method the integrity of the original image was preserved without smoothing effect. As a result the generated image after resampling had the same grid size, coordinate projection as that of the raster grid map

### 3.7.1.5 Spatial Modeler program to make single layer image

The *Spatial Modeler* program of ERDAS was used to make the 17 layers image in a single layer image. The program is a graphical modeling tool which is used to place the graphics representing input data, functions, criteria, and output data on a page by drawing its flow chart. Each of the layers except the seventeenth layer of both the files was having 100 as the maximum and 0 as minimum pixel value. The summation of multiplied values of each band with its band number and correspondingly dividing by 100 yielded the out put image as a single layer.

***Input:*** *17 layers stacked image*

***Function:***

$$\frac{\{\ \$n1\_stack(1)\times 1+\$n1\_stack(2)\times 2+\$n1\_stack(3)\times 3+\$n1\_stack(4)\times 4.....\$n1\_stack(17)\times 17\ \}}{100}$$

***Output:*** *Single layer image*

The program made the single layer out put image showing the pixel values ranging from zero to sixteen as the $17^{th}$ band is having no data. The unique pixel value in the output image corresponds to the retrospective soil type.

### 3.7.2 Soil Parameters

The significant soil parameters required by the VIC model for each soil layer are; saturated hydraulic conductivity, soil moisture diffusion parameter, soil particle density, bulk density, fraction of residual moisture content, fraction of soil moisture content at wilting point and fraction of soil moisture content at critical point and Brooks Corey exponent parameter in the Brooks-Corey equation for (Brooks and Corey, 1966). The parameter estimation was based on United States Department of Agriculture (USDA) soil texture classes. Apart from these the soil parameters including field capacity, wilting point and the maximum moisture content for each of the soil layers were also approximated for the study region. To workout the VIC soil parameters. These approximations and estimations are based on the work of *sample index of soil hydraulic properties* of given in Appendix A in Table A1.

**4 (a) Exponent (expt) parameter**

The exponent *(expt)* parameter is the exponent, n, from the Brooks-Corey relationship. It was obtained from the *b* parameter in which it represents the slope of the moisture retention curve, in log space, using the relation $n = 3 + 2b$ (Rawls *et al*. 1993).

$$n=3+2*b \quad \text{----------} \quad (3.1)$$

Where, b is the slope of the Retention Curve (in log space)

**5 (b) Saturated hydraulic conductivity parameter**

The parameter Ksat is the saturated hydraulic con has been estimated in mm/day using the Ksat values for USDA soil classes by using the unit transformation factor as 240.

*Ksat (mm/day) = Ksat (cm/hour) x 240* ----------(3.2)

**6 (c) Bulk density parameter**

The bulk density in layers used in the VIC model has been compiled for different soil type. The estimation were made in $kg/m^3$ ($g/cm^3$ x1000 = $kg/m^3$)

*Bulk density ($kg/m^3$) = Bulk density ($g/cm^3$) x 1000* --------- (3.3)

**(d)Particle density parameter**

The particle density ($kg/m^3$) for each soil type was estimated using the porosity values in the Appendix (A.1) and the calculated values of bulk density for each soil type.

$$\Phi = 1 - (BD / PD) \quad \text{----------} \quad (3.4)$$

*Where,*

$\Phi$ = *Total Porosity*

*BD = soil bulk density, $kg/m^3$*

*PD = particle density, $kg/m^3$*

**7 e) Maximum moisture content**

8 The maximum moisture content for each soil type of each layer has been calculated by multiplying the porosity fraction to the layer depth

9 $MMC\_1 = \Phi \times Layer\ depth\_1$---------- (3.5)

10 $MMC\_2 = \Phi \times Layer\ depth\_2$---------- (3.6)

*11 Where,*

$\Phi$ = *Total Porosity*

*12 MMC_1=maximum moisture content of top layer, m*

*13 MMC_2= maximum moisture content of bottom layer, m*

*14 Layer depth_1=depth of the top layer, m*

*15 Layer depth_2=depth of the bottom layer, m*

**16 (f) Field capacity**

Field capacity is defined as the water content at a tension of -33kPa. Field capacity for each of the soil type for each layer had been calculated from the described values field capacity in Appendix A Table A1 as a fraction of the maximum moisture content.

*FC_1= field capacity as the fraction of max. moisture content x MMC_1*------ (3.7)

*FC_2= field capacity as the fraction of max. moisture content x MMC_2* ---- (3.8)

Where,

*MMC_1=maximum moisture content of top layer, m*

*MMC_2= maximum moisture content of bottom layer, m*

*FC_1= field capacity for the top layer, m*

*FC_2= field capacity for the bottom layer, m*

**(g) Fractional soil moisture Parameter**

It is the fractional soil moisture expressed as a fraction of the maximum soil moisture at the critical point, which is the water content below which hydraulic conductivity begins to fall below saturated values, as does transpiration. The parameter values were calculated at 70% of the field capacity, in accordance with the different soil textures.

*Wcr_FRACT= field capacity as a fraction of max. soil moisture x 0.70* ---- (3.9)

*Where,*

*Wcr_FRACT =Wcr_FRACT is the fractional soil moisture*

**(h) Fractional soil moisture parameter at wilting point**

It is the fractional soil moisture expressed as a fraction of the maximum soil moisture at the wilting point. Wilting Point was considered at the water content at a tension of –1500 kPa, and approximated for the different soil textures.

*31 Wpwp_FRACT = wilting point as fraction of maximum moisture content*

**32 (i) Residual moisture Parameter (resid_moist)**

Residual moisture content is the amount of soil moisture that cannot be removed from the soil by drainage or evapotranspiration. When residual soil moisture is defined as 0 mm/mm the soil hydraulic conductivity relationship collapses to *Campbell* (1974), otherwise it follows *Brooks and Corey* (1964). The values have been obtained from Infiltration and soil water movement given by, handbook of hydrology by David.R..Maidment (1993)

**33 (j) Initial moisture parameter**

Initial moisture content of each layer can be set at any reasonable value for VIC model. One approach is to use fractional soil moisture content (expressed as a fraction of the maximum soil moisture; max. soil moisture = porosity x layer depth) at the critical point, Wcr, which were computed for each layer as a depth in mm by multiplying Wcr by the thickness of the layer in m, and then multiplying by 1000.

These parameters had been generated for the corresponding soil type using M.S. Excel package that also allowed in making the requisite calculations. The derived soil parameters are listed in Appendix A in Table A3 and Table A4.

However; several model parameters of VIC can't be determined based on the available soil information. These parameters need to be calibrated according to the basin selected for study. These are exponent of VIC curve which describes the spatial variability of soil moisture capacity and the parameters in the ARNO subsurface flow parameterization including *Dsmax* parameter, *Ds* parameter and Ws parameter.

**34 (a) b_infilt parameter**

The b_infilt parameter is the parameter used to describe the Variable Infiltration Curve represented by the equation:

$$I = I_m \ [1-(1-A)1/b)] \quad \text{---------- (3.10)}$$

Where,

*I=infiltration at any point,*

$I_m$ *= maximum infiltration,*

*A=fractional area for which infiltration is to be calculated,*

*b= infilt. parameter.*

This is typically a value that can be adjusted during the calibration of the VIC model. The parameter values ranges from $10^{-5}$ to 0.4. Higher values will produce more runoff. Parameter value "0.2" is often used as a starting value.

**35 (b) Dsmax parameter**

The parameter Dsmax is the maximum velocity of base flow in mm/day for each grid cell. This can be estimated using the saturated hydraulic conductivity, Ksat, for each grid cell multiplied by the slope of the grid cell

*i.e*. **Dsmax= hydraulic conductivity x slope of the grid cell**

The values for *Ksat* can be averaged for the layers for which base flow will be included. When working in decimal degrees, the elevation data for the basin should be projected to an equal area map projection, in order to have horizontal dimensions in the same units as the vertical dimensions so that the slopes computed in Arc/Info are meaningful values.

**36 (c) Ds parameter**

The soil parameter Ds represents the fraction of the *Dsmax* parameter at which non-linear base-flow occurs. This is typically a parameter that can be adjusted during the calibration of the VIC model. An initial value of 0.001 may be used. Typically this value is small (less than 1).

**37 (d) Ws parameter**

The parameter Ws is the fraction of maximum soil moisture where non-linear baseflow occurs. As with the *Ds* parameter, this is generally adjusted during the calibration phase of applying the VIC model. Values for Ws are typically greater than 0.5. An initial value of 0.9 can be used.

### 3.7.3 Generation of raster attribute maps for the soil parameters

Attributes are the descriptive information about features or elements of a database. In statistical parlance, an attribute is a "variable", whereas the database feature represents an "observation" of the variable. To make soil database for the VIC, the worked out soil parameters were linked to the generated soil maps by appending the parameters as the raster attributes. For each of the parameters the corresponding raster attribute maps had been generated in ILWIS. The steps involved while generating the raster attribute maps were;

**(a) Importing the generated soil map in the ILWIS software**

The generated soil maps in "*img.*" format was imported ILWIS3.2 as "*ILWIS*" data format using *PCI-Geo Gateway*.

**(b) Creating domain for the soil maps**

A domain defines the values, classes or identifiers that can be stored in a map. For creating the domain for the soil maps, the *Class type* domain was used, as it is suitable for thematic maps. The created domain was named as *soil_type*. Furthermore, the different soil types have been added as the classes for the domain.

**c) Making attribute table**

An attribute table functions as storage of additional information on elements in a map (extra tabular data which relates to the mapping units in maps). However, the domain is the relational link between map and the attribute table. Therefore, while creating the soil attribute table, its domain was kept the same as the soil *_type*. Using a value domain for each of the columns additional attribute information (in columns of the table) has been added for each of the classes of the soil map. Finally, using the raster option, in ILWIS raster attribute maps for each of the attributes were generated. These digital maps show the spatial variation of the parameters over the study area.

**3.8. Vegetation data set**

The vegetation data set is derived from classified land use/cover map of south central Asia at 1Km grid resolution. For each type of vegetation, parameters are based on information from Land Data Assimilation System (LDAS). http://ldas.gsfc.nasa.gov/.

### 3.8.1 Derivation of land use/cover data

Land use/cover has significant effects on hydrological processes, as it is the important factor in determining the water energy balances. Therefore, a comprehensive and standardized characterization of land use/cover is needed while driving any land surface model like VIC. Land use/cover map for the study region has been derived from the classified data of central south Asia, which was produced from the satellite SPOT satellite (*SPOT VEGETATION)* data using images for the time span 1999/2000.

The LLUC map was in geographic lat-long projection and it was having resolution much higher than that at which the VIC model could be applied (10 km). Moreover, the classified raster map is having 45 classes, conversely to the UMD vegetation classification having only 13 classes.

To generate the LULC in the required format the land cover map was re-projected from geographic lat/long to the Albers conical equal area projection in ERDAS. The re-projected map was resampled to 10 km X10 km grid size with total number of rows as 325 and total number of columns as 375.

The derived land use/cover data was having 45 classes, conversely to the dataset to be generated for the 13 UMD vegetation classes. The resample 45 class data was recoded to 13 classes using the *recode* function of ERDAS. While recoding; the various vegetation classification schemes were applied. Appendix B Table B.1 contains the recoding scheme used to generate 13 classes land use/cover data. Thus the LULC was generated according to the UMD vegetation classification, at model resolution in Albers conical equal area projection.

### 3.8.2 Vegetation parameters

The values of static UMD vegetation parameters required for the VIC model obtained from *table of LSM-based and observation-based vegetation parameters.* available at http://ldas.gsfc.nasa.gov/LDAS8th/MAPPED.VEG/web veg.table.html . The parameters extracted from the table included; rooting depth, over story flag, stomatal resistance. The values for architectural resistance ($R_{arc}$) are based on Ducoudre *et al.* (1993). in Appendix B.5.

On the other hand, the values of monthly UMD vegetation parameter required for the VIC model have been extracted from *Table of Mosaic-based monthly vegetation parameters which have been mapped to the UMD scheme* available on the web page http://ldas.gsfc.nasa.gov/LDAS8th/MAPPED.VEG/ web.veg.monthly.table.html. Variables extracted from the table for the VIC model were Leaf Area Index (LAI) and, the other monthly parameters including roughness length and displacement height were derived from the vegetation height.

(a) Leaf Area Index (LAI)

The leaf area index LAI is half the total green leaf area (one-sided area for broad leaves) in the plant canopy per unit ground area. LAI describes a fundamental property of the plant canopy in its interaction with the atmosphere, especially concerning radiation, energy, momentum and gas exchange. Leaf area plays a key role in the absorption of radiation, in the deposition of photosynthates during the diurnal and seasonal cycles, and in the pathways and rates of biogeochemical cycling within the canopy-soil system. It is a non-dimensional variable ($m^2/m^2$) and is one of

the vegetation parameters to which VIC model is most sensitive. It controls not only precipitation (solid and liquid) interception, but also canopy resistance to transpiration, and the attenuation of solar radiation through the vegetation cover.

**b) Albedo**

Albedo has large impact on VIC's computed evaporation from the canopy, and plant transpiration. As the ratio of the downwelling to upwelling shortwave radiative fluxes at the surface, surface albedo is fundamental to surface energy balance. It is one of the most important parameters modulating the earth's climate, especially over land. It undergoes considerable variation over space, and shows strong seasonal cycles and inter-annual variability *i.e.* region and time specific.

**c) Vegetation height, displacement height, roughness length, and architectural resistance**

Vegetation height is used by VIC as the basis for determining *roughness length* and *displacement height*, both of which are important parameters in its evapotranspiration formulation. *Roughness length* is defined as the height above the ground where wind speed is reduced to zero due to surface resistance. This parameter is used to determine the wind profile in VIC using a logarithmic approximation. *Displacement height* is defined as the heights above the ground where wind speed is not significantly affected by surface roughness. The values used for *architectural resistance* (*Rarc)* are based on Ducoudre *et al.* (1993).

Roughness length and displacement height were estimated by multiplying the vegetation height in Table 3 by the factors *0.123* and *0.67*, respectively).

38 *Roughness_Length = Vegetation_height x 0.123* ---------- (3.11)

39 *Vegetation displacement _height = Vegetation_height x 0.67* ------- (3.12)

**(d) Minimum stomatal resistance**

The minimum stomatal resistance is defined as that occurring with full sunlight and at saturation leaf water potential. VIC uses the parameter together with LAI and current soil moisture to calculate the canopy resistance to transpiration – based on the formulations of Blondin (1991) and Ducoudre et al. (1993), as described in Liang et al. (1994).

**(e) Wind and wind attenuation**

The VIC parameter *wind height* is the height above ground at which wind observations were recorded. The model expects this measurement to have been made at high enough elevation that the vegetation effects on wind speed are negligible, and then estimates wind speed through and below the canopy using typical logarithmic wind profiles. *Wind speed attenuation* through the overstory to a 2 m height could be approximated at 50% when a tree canopy is present and at 10% when it is not.

**(f) Maximum rooting depth**

Maximum rooting depth affects the ability of the vegetation to extract moisture from the specified soil layers of the model, and hence affects evapotranspiration, and the partitioning of precipitation into runoff and evapotranspiration. The values of maximum rooting depth values for the data set were listed in Table 4.14.

**3.8.3 Generation of raster data for the vegetation parameters**

To make vegetation dataset for the VIC, the worked out vegetation parameters were linked to the generated soil maps by appending the parameters as the raster attributes. For each of the parameters the corresponding raster attribute maps had been generated in ILWIS. The steps involved while generating the raster attribute maps;

**(a) Importing the generated land use/cover data in the ILWIS:**

The derived land use/cover data for UMD vegetation classes in "*img."* format was imported in ILWIS as "ILWIS.*"* data format using *PCI-Geo Gateway*.

**(b)Creating Domain for the vegetation parameters**

For creating the domain for the vegetation parameters, the *class type* domain was used. The created domain was named as *vegetation type*. Furthermore, the different vegetation types were added as the classes for the domain.

**(c) Making attribute table**

While creating the vegetation attribute table, its domain was kept the same as the *vegetation type*. Using a value domain for each of the columns additional attribute information were added for each of the classes of the land use/cover data.

Finally, using the raster option, raster attribute maps for each of the attributes were generated.

**3.9 Topographic dataset generation**

The topographic dataset required for the VIC model were derived from *GTOPO 30*, Global 30 Arc Second Elevation data. The derived data included the DEM and slope data for the study region.

### 3.9.1 DEM extraction from GTOPO 30 data

The Digital Elevation Model (DEM) is a digital representation of continuous variation of elevation over space; it provides a base dataset from which topographic parameters can be digitally generated. In fact, it is the principal digital data source for generation of slope and aspect map coverage used in geographic information system (GIS) analysis. The DEM for the study region has been extracted from the tiles E060N40 and E100N40 of GTOPO30 data shown in Plate 3.2. The information regarding the tiles is shown in Table 3.7

**Table 3.7: GTOPO 30 tiles used for DEM extraction**

| Tile | Latitude | | Longitude | | Elevation | | |
|---|---|---|---|---|---|---|---|
| | Minimum | Maximum | Minimum | Maximum | Minimum | Maximum | Mean |
| E060N40 | -10 | 40 | 60 | 100 | 1 | 8752 | 1804 |
| E100N40 | -10 | 40 | 100 | 140 | -40 | 7213 | 692 |

The *3dem* software used for the DEM extraction, which has capability to produce the terrain images of the desired geographic extent by setting the central latitude, central longitude and the width of the terrain scenes. Likewise, for the six terrain images were extracted and saved in "*GeoTiff."* format. The geographic extent of each of the produced terrain images is given in Table 3.8.

**Table 3.8: Terrain scenes produced using *3dem* software**

| Terrain Scene | Longitude-Range | Latitude - Range |
|---|---|---|
| Ind_1 | 100-120 | 0.0-20 |
| Ind_2 | 100-120 | 20-40 |
| Ind_3 | 80-100 | 0.0-20 |
| Ind_4 | 80-100 | 20-40 |
| Ind_5 | 60-80 | 0.0-20 |
| Ind_6 | 60-80 | 20-40 |

Further more all the terrain scenes were imported in ENVI. The *mosaic program* of ENVI was used to merge the terrain scenes to make the cohesive image of the region having the geographic extent from 60° to 120°E longitude to 0° to 40°N latitude.

**3.9.1.1 Geo-referencing of the Mosiacked image in *geographic lat/long.***

As the mosiacked image didn't show any projection, it had been imported in ERDAS as "img." format for geo-referencing. Since the global DEM having the latitude extent from 90°S to 90°N and longitude extent from 180°W to 180°E, which implies that the data is having 21,600 samples and 43,200 lines. At parallence with it, the lines and samples values of the corner pixels of the mosiacked image were worked out.

The mosiacked image was made geo-referenced using the key*board function* by considering the calculated values of samples and lines of corner pixels as the source coordinate and the corresponding values of lat-long as the reference coordinate. While geo-referencing the geometric model was set as polynomial of first order transformation and projection system at Geographic lat/long with datum and spheroid as WGS 84.

### 3.9.1.2 Geo-referencing of the mosiacked image in *Albers conical equal area projection*

Once the mosiacked image got geo-referenced with geographic lat/long projection, the values of samples and lines corresponding to lat/ long positions of the corner pixels of the raster grid map (base map) were worked out as shown in Table 3.9.

**Table 3.9: Corner position of mosiacked image used for georeferencing**

| Corner position of raster grid map | Geographic Coordinate in mosiacked image | Corresponding Samples/Lines values in mosiacked image |
|---|---|---|
| ULY | Lat: 37˚ 20' 5.85", | Y:381 |
| ULX | Long:65˚ 57' 44.48" | X:682 |
| URY | Lat:36˚ 07' 30.25" | Y:464 |
| URX | Lat:100˚ 45' 30.54" | X:4877 |
| LLY | Lat:3˚ 06' 43.7" | Y:4416 |
| LLX | Long:68˚ 04' 36.2" | X:969 |
| LRY | Lat:2˚ 20' 40.07" | Y:4505 |
| LRX | Long:98˚ 23' 17.82" | X:4357 |

The worked out values of samples and lines were further used to georeference the mosiacked image with reference to the raster grid map. While geo-referencing the geometric model was set the same *i.e.* polynomial with first order transformation but the projection system was set at Albers conical equal area projection. Using the keyboard function in ERDAS the mosiacked image (without projection) was again geo-referenced by using the worked out sample and line values for the corner pixels of the raster grid map as the source coordinate.

#### 3.9.1.3 Resampling of mosiacked DEM using nearest neighbor

The derived DEM is further resampled to make the dataset according to the raster grid map by merely keeping the grid size, the lower left and upper left x-y coordinate same as the raster grid map. The layout of the derived DEM at Albers conical projection with 10 km resolution for the study region is shown in Plate 4.1.

### 3.9.2 Slope Generation from the raster DEM

Slope identifies the steepest downhill slope for a location on a surface. The per cent slope values were derived from the assimilated raster DEM data using the *3D Analyst* function of Arc Map. It made the point to Surface Analysis using raster DEM by calculating the maximum rate of change in elevation over each cell and its eight neighbors. The layout of the generated slope data is shown in Plate 4.2.

# CHAPTER IV
# RESULTS AND DISCUSSION

The chapter deals with the results of the present research work, which are confined to generation of soil, vegetation and topographic data sets primarily for Indian basins and a part of its subcontinent. The virtues of the generated data sets are at the model grid resolution of (10 x 10 km) in Albers conical equal area projection. The corresponding ASCII format of the datasets has been generated, which serves as the input for macroscale hydrologic based Variable Infiltration Capacity (VIC-2l) land

## 4.1Topographic Dataset

For topographic analysis the DEM was aggregated from freely available *30 arc second resolution USGS GTOPO30 Data.* The downloaded data had been processed through *3-DEM software* to create multiple terrain scenes. Using the image processing and GIS analysis software, the data was retransformed to the desired projection and resolution as explained in Section (3.9.1) of Chapter III. The extracted DEM is shown in Plate 4.1, which saliently defines the elevation range in terms of the bedraggled colours. The statistical representation of elevation data is shown in Fig.4.1. The wide variation in elevation was observed from mere 0 m to as high as 8593 m. The areal coverage of each of the elevation range is mentioned in Table 4.1. The majority of the pie is acquired by the sea region which is about 5132600 $km^2$. At the same time the zone of highest elevation range is noticed *i.e.* the Himalayan region having the mere coverage of 600 $km^2$ area.

**Table 4.1: Pixels distribution of the DEM data**

| Elevation range(m) | No.of Pixel | Area($km^2$) |
|---|---|---|
| 0 | 51326 | 5132600 |
| 0-1 | 415 | 41500 |
| 1-100 | 10369 | 1036900 |
| 100-200 | 7671 | 767100 |
| 200-500 | 14134 | 1413400 |

| | | |
|---|---|---|
| 500-1000 | 8235 | 823500 |
| 1000-1500 | 2690 | 269000 |
| 1500-2000 | 1978 | 197800 |
| 2000-3000 | 3070 | 307000 |
| 3000-4000 | 2886 | 288600 |
| 4000-5000 | 12016 | 1201600 |
| 5000-6000 | 6909 | 690900 |
| 6000-7000 | 170 | 17000 |
| 7000-8593 | 6 | 600 |
| Total | 121875 | 12187500 |

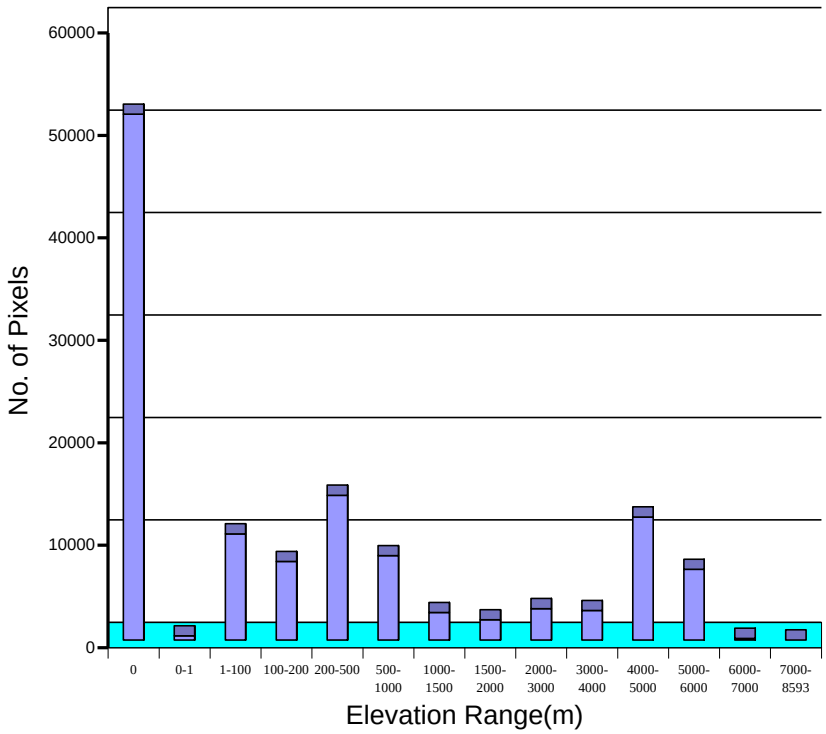


**Figure 4.1: Pixel distribution with respect to the elevation range of the DEM**

Using the extracted DEM corresponding per cent slope was generated in Arc Map. Plate 4.2 shows the spatial variation of of percent slope for the region, which ranges from 0 to 21.7 % for the entire region. The topographic parameter is significant for calculation of the *Dsmax* , one of the parameter for the model.

**Topographic Datset files:**

**Structure:**

1. Raster data file: 10000m *Albers conical equal area* (false easting /false northing)
   375x325 grid
2. ASCII file

**System Files:**

| File type | Metadata | Data |
|---|---|---|
| Raster grid | Ind_topo.doc | Ind_dem.img |
| | | Ind_slope.img |
| ASCII file | | Ind_dem.asc |
| | | Ind_slope.asc |
| Attribute Table | Ind_topo.xls | |

### 4.2 Generation of Digital Soil Datasets

The elements of the datasets primarily are the hydrologic soil parameters required for the model. However in due course of the dataset generation, soil map for both the soil layers (0-30cm and 30-100cm) were generated, followed by parameter derivation and finally the raster attribute map generation as explained in Section 3.7.1 of ChapterIII. The ASCII file format of the generated data serves as the model input. The Section 3.7.2 of the Chapter III explains the generated soil maps and the corresponding raster data of the soil parameters.

#### 4.2.1 Extraction of soil texture data

The soil texture data for the two-layer soil depth have been extracted using the global coverage *MM5 V3 Terrain data* which is further based on *FAO* and *STATSGO*

soil data. Layouts of the extracted soil texture data for the retrospective layer depths are shown in Plate (4.3) and the Plate (4.4). Fig. 4.2 shows the spatial variation of the soil data for both of the soil layers. The corresponding areal coverage and pixel distribution are mentioned in Table 4.2. The numerical interpretation of the pixel data reveals that the soil type including silt, silt clay loam, sandy clay, silty clay, organic material and bedrock have no coverage in the upper layer. At the same time loam sand texture covers just 100 $km^2$ and the sandy soil covers mere 6400 $km^2$ area. In contrast, the loam soil is dominant soil type in the region with the total 3615600 $km^2$, followed by the clay loam and the clay type soil texture.

**A (0-30cm depth)** **B (30-100cm depth)**

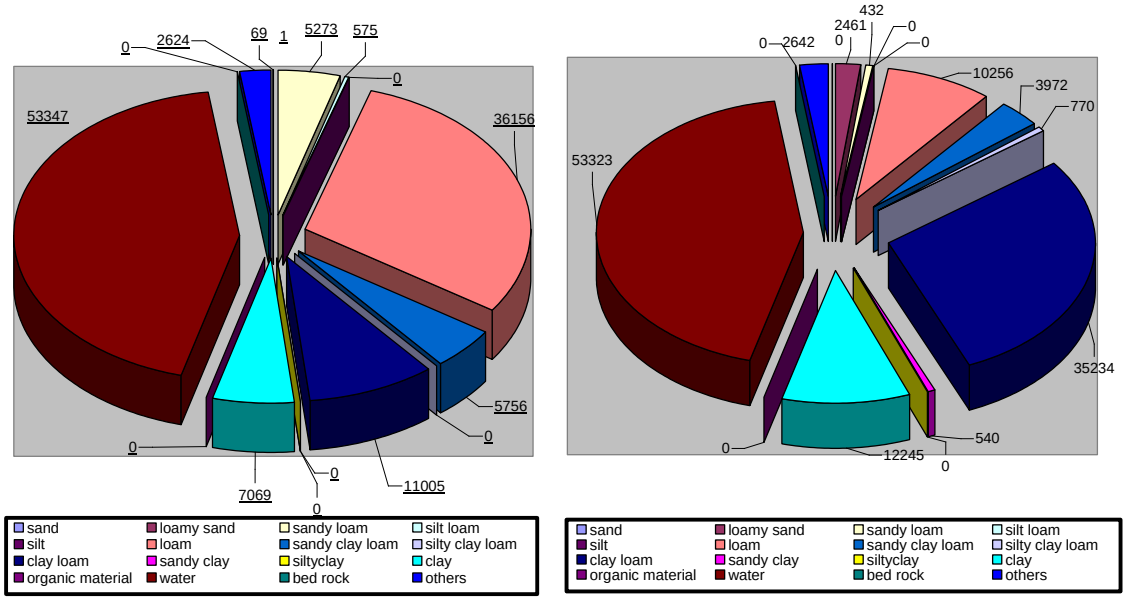


**Figure 4.2: Spatial variation of soil texture data**

Moreover, the lower soil profile for (30-100cm) depth shows entirely different soil texture distribution for the region. The soil texture including; sand, silt loam, silt, silty clay, bed rock and organic material shows no coverage in the data. However, the

dominant soil type is the clay loam soil with areal coverage 3523400 $km^2$ followed by clay and loam type soil texture.

**Table 4.2: Pixel distribution of soil texture data**

**A (0-30cm depth)**

| Soil Type | No. Pixels | Area($km^{2)}$ |
|---|---|---|
| Sand | 69 | 6900 |
| Loamy sand | 1 | 100 |
| Sandy loam | 5273 | 527300 |
| Silt loam | 575 | 57500 |
| Silt | 0 | 0 |
| Loam | 36156 | 3615600 |
| Sandy clay loam | 5756 | 575600 |
| Silty clay loam | 0 | 0 |
| Clay loam | 11005 | 1100500 |
| Sandy clay | 0 | 0 |
| Silty clay | 0 | 0 |
| Clay | 7069 | 706900 |
| Organic material | 0 | 0 |
| Water | 53347 | 5334700 |
| Bed rock | 0 | 0 |
| Others | 2624 | 262400 |
| Total | 121875 | 12187500 |

**B (30-100cm depth)**

| Soil Type | No. Pixels | Area($km^2$) |
|---|---|---|
| Sand | 0 | 0 |
| Loamy sand | 2461 | 246100 |
| Sandy loam | 432 | 43200 |
| Silt loam | 0 | 0 |
| Silt | 0 | 0 |
| Loam | 10256 | 1025600 |
| Sandy clay loam | 3972 | 397200 |
| Silty clay loam | 770 | 77000 |
| clay loam | 35234 | 3523400 |
| sandy clay | 540 | 54000 |
| Silty clay | 0 | 0 |
| Clay | 12245 | 1224500 |
| Organic material | 0 | 0 |
| Water | 53323 | 5332300 |
| Bed rock | 0 | 0 |
| Others | 2642 | 264200 |
| Total | 121875 | 12187500 |

At the same time, the water distribution over both the soil layer differs by 2400 $km^2$. The upper horizon shows the higher distribution of water because of the surface water.

### 4.2.2 Soil Prameters

The different representative soil properties were worked out corresponding to the USDA soil texture classes for the two-layer depths (0-30 and 30-100 cm) of the soil profile. The generated soil parameters required for the VIC model were

linked to the generated texture data as explained in Section 3.7.2 of Chapter III. The corresponding raster data for each of the attributes were generated. The visual and statistical interpretation of significant parameters including soil parameters have been analyzed in the section. These raster datasets include *saturated hydraulic conductivity, Brooks' Corey exponent parameter, soil particle density, bulk density, fraction of residual moisture content,* fraction *of soil moisture content at wilting point* and fraction *of soil moisture content at critical point.*

***1. Brooks-Corey exponent parameter (expt)***

The variation of the Brooks-Corey exponent, n, were estimated from the slope of the Retention Curve (in log space), as explained in Section 3.7.2.

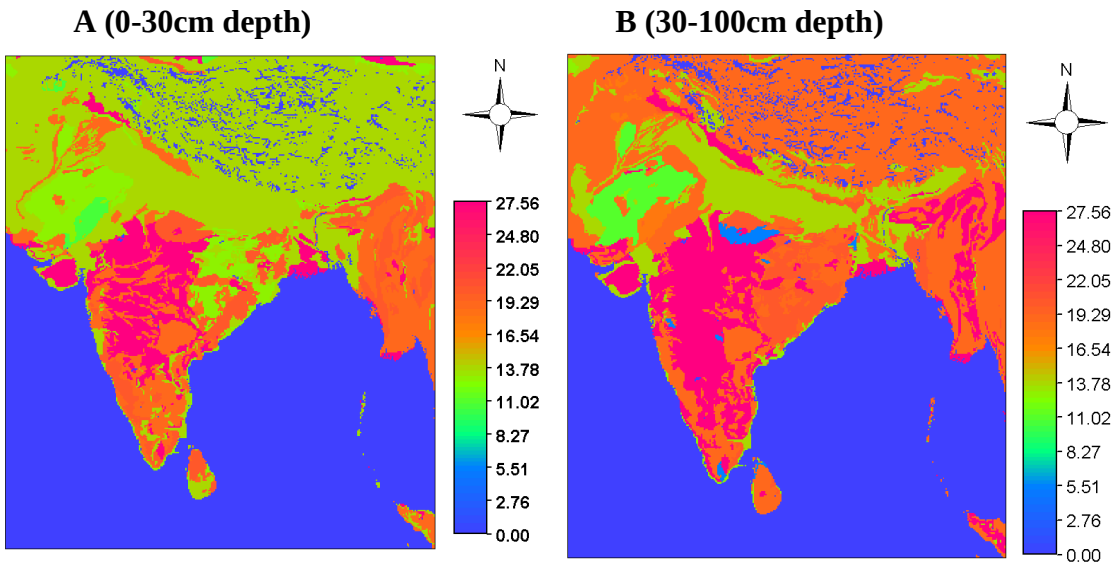


**Plate 4.5: Brook's Corey Exponent parameter**

.

**Table 4.3: Pixel distribution of Brook's Corey Exponent parameter**

| A (0-30cm depth) | | | | B (30-100cm depth) | | |
|---|---|---|---|---|---|---|
| **Value** | **No. Pixels** | **Area($km^2$)** | | **Value** | **No. Pixels** | **Area($km^2$)** |
| 0 | 55971 | 5597100 | | 0 | 55965 | 5596500 |
| 10.58 | 575 | 57500 | | 5.6 | 540 | 54000 |
| 10.98 | 1 | 100 | | 10.98 | 2461 | 246100 |
| 11.2 | 69 | 6900 | | 12.68 | 432 | 43200 |
| 12.68 | 5273 | 527300 | | 13.6 | 10256 | 1025600 |
| 13.6 | 36156 | 3615600 | | 17.96 | 770 | 77000 |
| 19.04 | 11005 | 1100500 | | 19.04 | 35234 | 3523400 |
| 20.32 | 5756 | 575600 | | 20.32 | 3972 | 397200 |
| 27.56 | 7069 | 706900 | | 27.56 | 12245 | 1224500 |
| **Total** | **121875** | **12187500** | | **Total** | **121875** | **12187500** |

The spatial variation of Brook Corey exponent parameter is shown in Plate 4.5 for the retrospective soil layers. These show the variation of the parameter according to the soil texture The pixel distribution and areal coverage of the raster data are given in Table 4.3. The parameter variation for the defined domain of top soil ranges from 10.58 to 27.56, whereas for the bottom layer shows the variation from 5.6 to 27.56. Moreover, the parameter value 13.6 corresponds to the maximum areal coverage in top soil layer, while the value 19.04 shows dominance in lower layer.

***2. Saturated hydraulic conductivity (Ksat)***

The Ksat parameter was estimated for both of the soil layers to be used in VIC-2l mode in mm/day. The spatial variation of the hydraulic conductivity for both the soil layers is depicted in Plate 4.6.

The dataset element for the defined domain shows variation from 428.8 to 9218.4 mm/day for the upper soil profile and 285.6 to 2608 mm/day for the lower profile.

**Table 4.4: Pixel distribution of saturated hydraulic conductivity**

**A (0-30cm depth)**

| Value (mm/day) | No. Pixels | Area($km^2$) |
|---|---|---|
| 0 | 55971 | 5597100 |
| 424.8 | 11005 | 1100500 |
| 472.8 | 36156 | 3615600 |
| 576 | 5756 | 575600 |
| 763.2 | 7069 | 706900 |
| 950.4 | 575 | 57500 |
| 1257.6 | 5273 | 527300 |
| 2608.8 | 1 | 100 |
| 9218.4 | 69 | 6900 |
| Total | 121875 | 12187500 |

**B (30-100cm depth)**

| Value (mm/day) | No. Pixels | Area($km^2$) |
|---|---|---|
| 0 | 55965 | 5596500 |
| 285.6 | 540 | 54000 |
| 424.8 | 35234 | 3523400 |
| 472.8 | 10256 | 1025600 |
| 576 | 3972 | 397200 |
| 763.2 | 12245 | 1224500 |
| 1096.8 | 770 | 77000 |
| 1257.6 | 432 | 43200 |
| 2608.8 | 2461 | 246100 |
| Total | 121875 | 12187500 |

The pixel-area coverage of the data for the retrospective soil depth is presented in Table 4.4. The zero hydraulic conductivity includes the surface coverage including the water body as well as the soil type for which the parameter is not defined.

**A (0-30cm depth)** **B (30-100cm depth)**

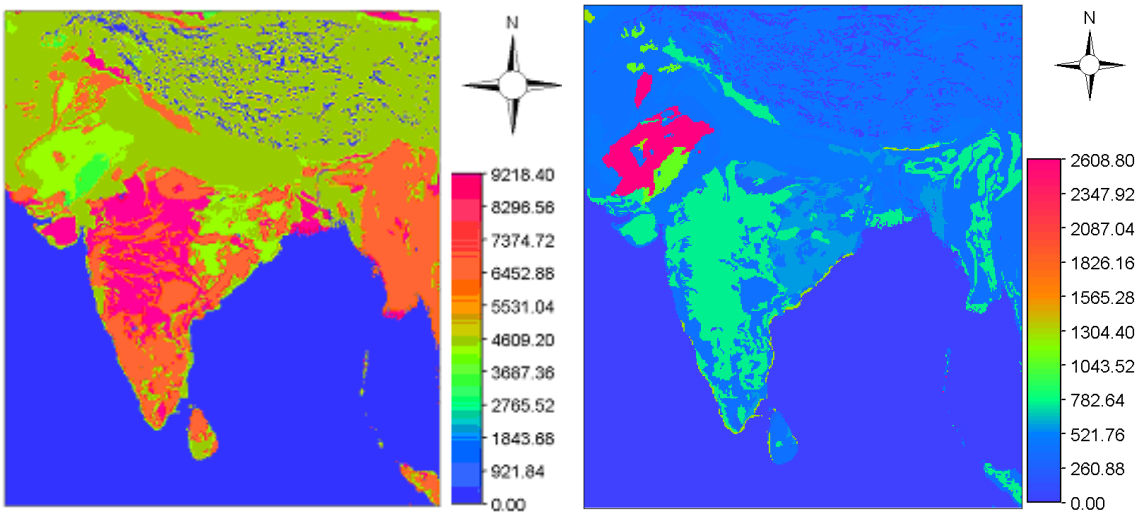


**Plate 4.6: Saturated hydraulic conductivity (mm/day)**

***3. Soil particle density (soil_desity)***

The model parameter was worked out in kg/m$^3$ with refernce to the known porosity and bulk desity, as explained in Section 3.7.2 of Chapter III. The spatial variation of the generated datset element is shown in Plate 4.7.

**Table 4.5: Pixel Distribution of soil particle density of the soil layers**

**A (0-30cm depth)**

| Value (kg/m$^3$) | No. Pixels | Area(km$^2$) |
|---|---|---|
| 2614.035 | 36225 | 3622500 |
| 2616.667 | 5273 | 527300 |
| 2620.69 | 1 | 100 |
| 2622.642 | 7069 | 706900 |
| 2622.951 | 5756 | 575600 |
| 2629.63 | 575 | 57500 |
| 2648.148 | 11005 | 1100500 |
| | | |
| Total | 65904 | 6590400 |

**B (30-100cm depth)**

| Value (kg/m$^3$) | No. Pixels | Area(km$^2$) |
|---|---|---|
| 2614.035 | 10256 | 1025600 |
| 2616.667 | 432 | 43200 |
| 2620.69 | 2461 | 246100 |
| 2622.642 | 12245 | 1224500 |
| 2622.951 | 3972 | 397200 |
| 2648.148 | 35234 | 3523400 |
| 2653.846 | 770 | 77000 |
| 2661.017 | 540 | 54000 |
| Total | 65910 | 6591000 |

**A (0-30cm depth)** **B (30-100cm depth)**

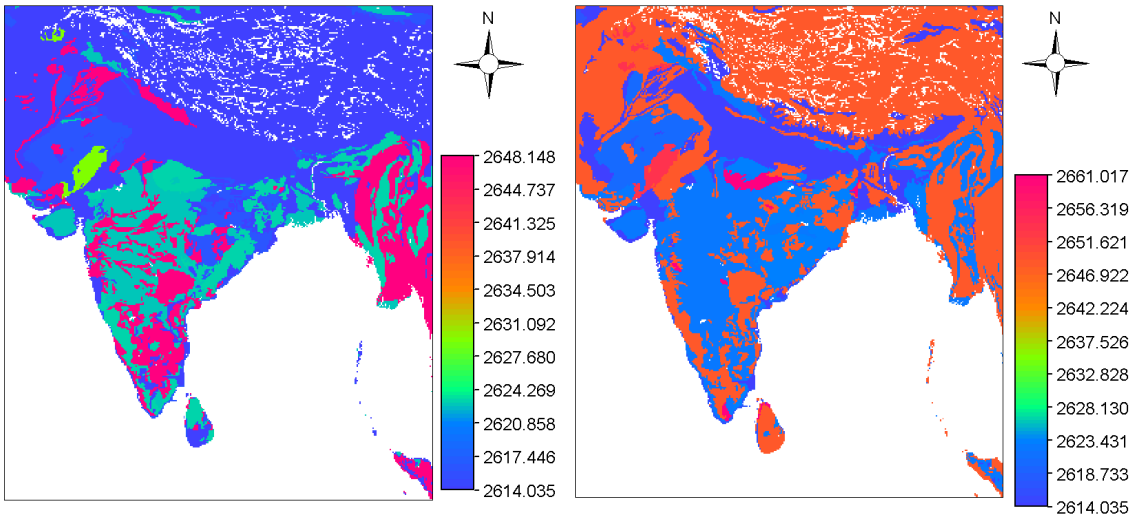


**Plate 4.7: Soil particle density parameter (kg/m$^3$)**

The soil density variation ranges from 2614.03 to 2648.14 for the upper soil layer, where as lower soil profile shows the variation from 2614.03 to 2661.017 kg/m$^3$.

However the spatial distribution of pixels for the defined domain of the parameter differs significantly as shown in Table 4.5. The upper soil horizon is defined for 6590400 km$^2$ of whereas the the lower profile is for 6591000 km$^2$

***4. Soil bulk desity (bulk_desity):***

The significant soil parameter for the VIC model was estimated in kg/m$^3$ using *Schaake's* table as explained in Section 3.7.2 of Chapter III. The layout of the generated dataset is shown in Plate 4.8.

**A (0-30cm depth)** **B (30-100cm depth)**

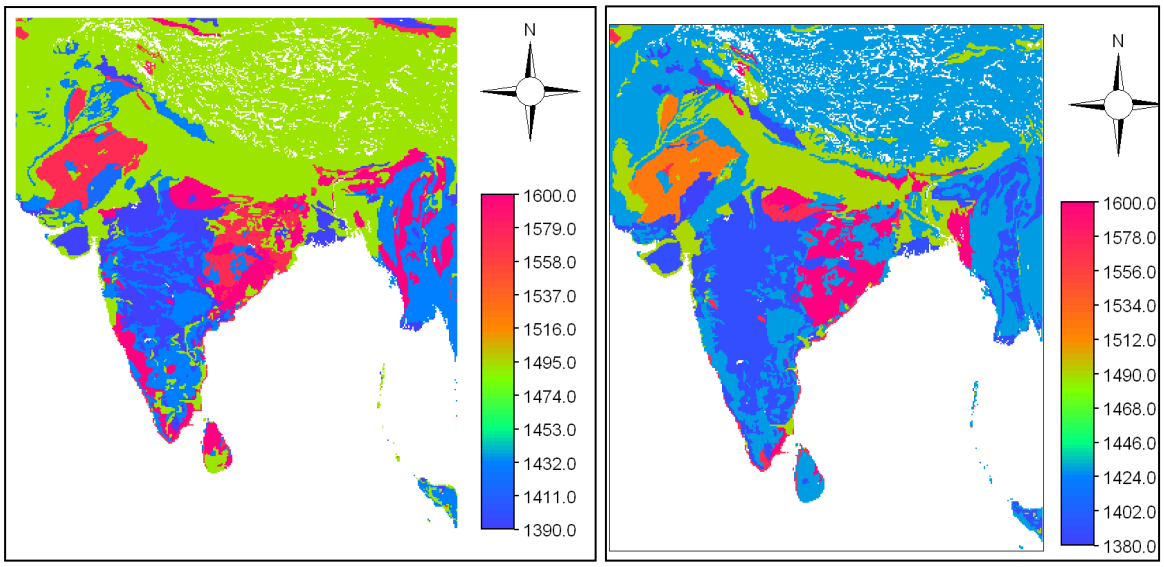


**Plate 4.8: Soil bulk density parameter (kg/m$^3$) of soil layers**

It shows the spatial variation of bulk desity for the defined domain of the retrospective soil layers. The data ranges from 1390 to 1600 kg/m$^3$ for the upper soil profile whereas the lower profile ranges from 1380 to 1600 kg/m$^3$. Pixels distribution and the corresponding areal coverage for the layers are shown in Table 4.6. The parameter is defined the upper soil horizon is defined for 65904 pixels of the upper layer depth and 65910 pixels for the lower depth profile.

**Table 4.6: Soil bulk density parameter**

**A (0-30cm depth)**

| Bulk density (0-30cm depth) | | |
|---|---|---|
| Value (kg/m$^3$) | No. Pixels | Area(km$^2$) |
| 1390 | 7069 | 706900 |
| 1420 | 575 | 57500 |
| 1430 | 11005 | 1100500 |
| 1490 | 36225 | 3622500 |
| 1520 | 1 | 100 |
| 1570 | 5273 | 527300 |
| 1600 | 5756 | 575600 |

**B (30-100cm depth)**

| Bulk density (30-100cm depth) | | |
|---|---|---|
| Value (kg/m$^3$) | No. Pixels | Area(km$^2$) |
| 1380 | 770 | 77000 |
| 1390 | 12245 | 1224500 |
| 1430 | 35234 | 3523400 |
| 1490 | 10256 | 1025600 |
| 1520 | 2461 | 246100 |
| 1570 | 972 | 97200 |
| 1600 | 3972 | 397200 |

| | | |
|---|---|---|
| Total | 65904 | 6590400 |

| | | |
|---|---|---|
| Total | 65910 | 6591000 |

***5. Fractional soil moisture content at critical point (Wcr_Fract):***

Fraction of soil moisture content at critical point (Wcr_Fract) is one of the parameter of VIC model, which is the defined as the the fraction of maximum soil moisture at 70% of field capacity as explained in Section 3.7.2.

**A (0-30cm depth)** **B (30-100cm depth)**

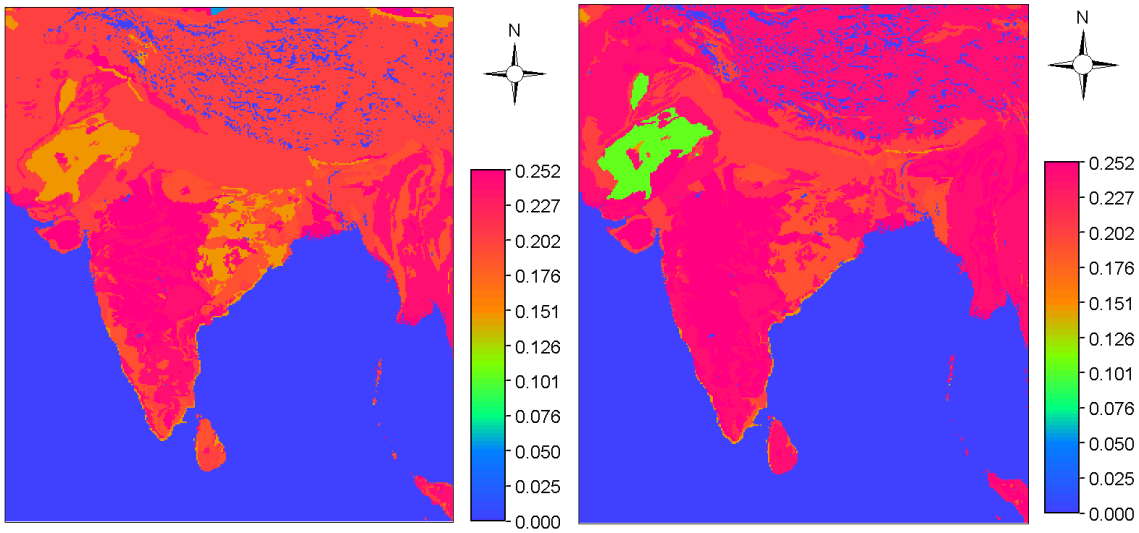


**Plate 4.9: Fractional soil moisture content at critical point (*Wcr_Fract)*)**

The layout of the dataset element, *Wcr_Fract* is depicted in Plate 4.9 for the respective soil layers. The spatial variation of the parameter ranges from 0.00 to 0.252 for both the soil layers. However, soil heterogeneities play important role in soil moisture distribution. The value range and the areal coverage of the parameter are given in Table 4.7.

**Table 4.7: Fractional soil moisture content at critical point**

| Value (fraction) | No. Pixels | Area($km^2$) |
|---|---|---|

| Value (fraction) | No. Pixels | Area($km^2$) |
|---|---|---|

| | | |
|---|---|---|
| 0 | 55971 | 5597100 |
| 0.056 | 69 | 6900 |
| 0.105 | 1 | 100 |
| 0.147 | 5273 | 527300 |
| 0.189 | 5756 | 575600 |
| 0.203 | 36156 | 3615600 |
| 0.224 | 575 | 57500 |
| 0.238 | 11005 | 1100500 |
| 0.252 | 7069 | 706900 |
| Total | 121875 | 12187500 |

**A (0-30cm depth)**

| | | |
|---|---|---|
| 0 | 55965 | 5596500 |
| 0.105 | 2461 | 246100 |
| 0.147 | 432 | 43200 |
| 0.189 | 3972 | 397200 |
| 0.203 | 10256 | 1025600 |
| 0.217 | 540 | 54000 |
| 0.238 | 35234 | 3523400 |
| 0.252 | 13015 | 1301500 |
| Total | 121875 | 12187500 |
| | | |

**B (30-100cm depth)**

***6. Fractional soil moisture content at wilting point (Wpwp_ Fract)***

The wilting point as a fraction of maximum moisture content (*Wpwp_ Fract*) for the VIC model was estimated for both the soil layers. The Plate 4.10 represents the layout of the generated data, which saliently defines the spatial variation of the parameter over the soil horizons.

The more lucid presentation of the pixel distribution and their areal coverage are listed in Table 4.8. The dominant value of 0.14 represents the loam texture of upper depth soil profile with total areal coverage of 3625600km$^2$.

**Table 4.8: Fractional soil moisture content at wilting point**

**A (0-30cm depth)**

| **Wpp-FRACT (0-30cm depth)** | | |
|---|---|---|
| Value (fraction) | No. Pixels | Area(km$^2$) |
| 0 | 55971 | 5597100 |
| 0.03 | 69 | 6900 |

**B (30-100cm depth)**

| **Wpp_FRACT (30-100cm depth)** | | |
|---|---|---|
| Value (fraction ) | No. Pixels | Area(km$^2$) |
| 0 | 55965 | 5596500 |
| 0.06 | 2461 | 246100 |

| | | |
|---|---|---|
| 0.06 | 1 | 100 |
| 0.09 | 5273 | 527300 |
| 0.12 | 575 | 57500 |
| 0.14 | 36156 | 3615600 |
| 0.17 | 5756 | 575600 |
| 0.21 | 11005 | 1100500 |
| 0.27 | 7069 | 706900 |
| Total | 121875 | 12187500 |

| | | |
|---|---|---|
| 0.09 | 432 | 43200 |
| 0.14 | 10256 | 1025600 |
| 0.17 | 3972 | 397200 |
| 0.21 | 36004 | 3600400 |
| 0.23 | 540 | 54000 |
| 0.27 | 12245 | 1224500 |
| Total | 121875 | 12187500 |
| | | |

**A (0-30cm depth)** **B (30-100cm depth)**

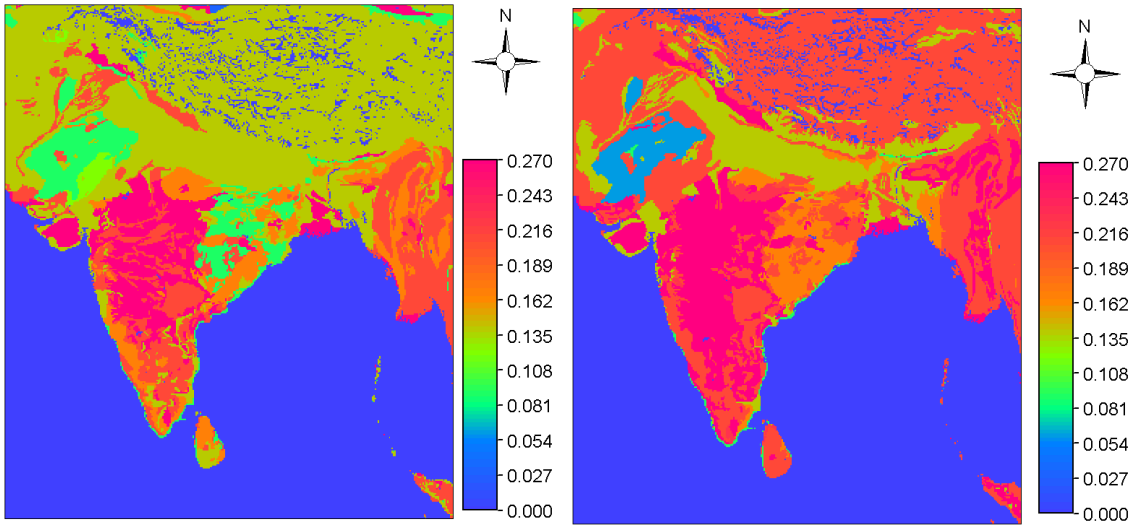


**Plate 4.10: Fractional soil moisture content at wilting point (Wpwp_Fract)**

Whereas, for the lower depth profile the value 0.21 corresponding to clay loam and silty clay loam shows the highest distribution over the region. Moreover, the maximum value of *Wpwp _Fract i.e. 0.*27 certifies the maximum retention of water in clay soil. Conversely, the least value of the parameter in the defined domain i.e. 0.03 signifies the presence of sandy soil in upper part of the soil horizon.

***7. Residual soil moisture fraction (resid_moist)***

Quantification of fractional variation of residual volume of soil moister with respect to the total volume of soil (*resid_moist)* plays indispensable role in soil water movement across the soil layers. The values are obtained for the corresponding USDA the raster data for the two soil layers. soil texture as explained in Section 3.7.2. Plate11 shows the spatial variation of. The fractional value of the parameter ranges from 0 to 0.09 for the upper soil horizon, whereas the the lower soil prfile shows the variation from 0.0 to 0.109.

**A (0-30cm depth)** **B (30-100cm depth)**

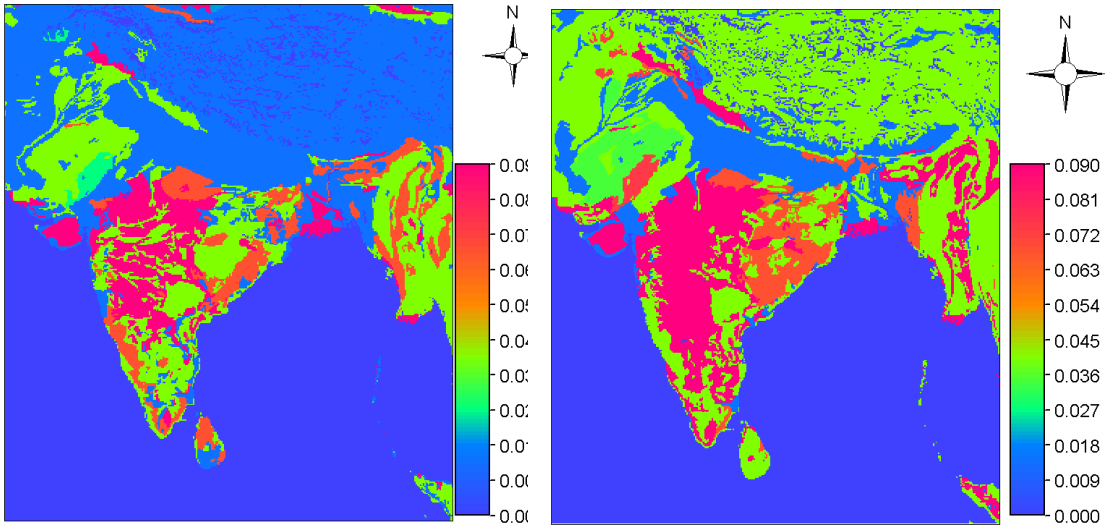


**Plate 4.11: Residual moisture fraction parameter**

The pixel distribution and the corresponding areal coverage are shown in Table 4.9. It is evident that the parameter value 0.015 shows the the maximum areal

coverage in upper soil horizon, whereas the value 0.04 shows the dominant coverage in the lower profile.

**Table 4.9: Pixel distribution of residual moisture fraction**

**A (0-30cm depth)**

| Value | No. Pixels | Area($km^2$) |
|---|---|---|
| 0 | 55971 | 5597100 |
| 0.015 | 36156 | 3615600 |
| 0.02 | 69 | 6900 |
| 0.027 | 575 | 57500 |
| 0.035 | 1 | 100 |
| 0.04 | 11005 | 1100500 |
| 0.041 | 5273 | 527300 |
| 0.068 | 5756 | 575600 |
| 0.09 | 7069 | 706900 |
| Total | 121875 | 12187500 |

**B (30-100cm depth)**

| Value | No. Pixels | Area($km^2$) |
|---|---|---|
| 0 | 55965 | 5596500 |
| 0.015 | 10256 | 1025600 |
| 0.035 | 2461 | 246100 |
| 0.04 | 35234 | 3523400 |
| 0.041 | 432 | 43200 |
| 0.068 | 3972 | 397200 |
| 0.075 | 770 | 77000 |
| 0.09 | 12245 | 1224500 |
| 0.109 | 540 | 54000 |
| Total | 121875 | 12187500 |

**39.1.1**

**39.1.2 Soil parameter file**

## 39.1.2.1 Structure:

39.1.2.2 For each of the raster data file corresponding ASCII file format has been generated

1. Raster data file: *10000m. Albers conical equal area (false Easting /false Northing) 375x325 grid*

2. ASCII files:

**39.1.2.3**

**39.1.2.4**

**39.1.2.5**

**39.1.2.6**

### 39.1.2.7 System Files:

| File type | Metadata | Data |
|---|---|---|
| Raster grid | Soil_param.doc | *Expt_A.img*<br>*Expt_B.img* |
| | | *Ksat_* A.img<br>*Ksat*_B.img |
| | | *soil_density* A.img<br>*soil_density* B.img |
| | | *bulk_desity* A.img<br>*bulk_desity* B.img |
| | | *Wcr_Fract* A.img<br>*Wcr_Fract* B.img |
| | | *Wpwp_ Fract* A.img<br>*Wcr_Fract* B.img |
| | | *resid_moist* A.img<br>*resid_moist* B.img |
| ASCII | | *Expt_A.asc*<br>*Expt_B.asc* |
| | | *Ksat_* A. *asc*<br>*Ksat*_B. *asc* |
| | | *soil_density* A. *asi*<br>*soil_density* B. *asc* |
| | | *bulk_desity* A. *asc*<br>*bulk_desity* B. *asc* |
| | | *Wcr_Fract* A. *asc*<br>*Wcr_Fract* B. *asc* |
| | | *Wpwp_ Fract* A. *asc*<br>*Wcr_Fract* B. *asc* |
| | | *resid_moist* A. *asc*<br>*resid_moist* B. *asc* |

| | | |
|---|---|---|
| Attribute Table | Soil_param.xls | |

### 4.3 Derivation of Land use/ cover data

The land use / cover data for the study region was derived from the 45 class land use cover data of central south Asia as described in Section 3.8 of ChapterIII. The data was initially reprojected in Albers conical projection, upscaled from 1 km to 10 km grid resolution and finally recoded according to the 13 UMD vegetation classes. Plate 4.12 shows the spatial variation of the UMD vegetation classes of the derived land use/cover data. Table 4.10 shows the spatial distribution and the corresponding areal coverage for the different vegetation type.

**Table 4.10: UMD vegetation classes in assimilated Land use/cover data**

| **UMD Vegetation Classes** | **No. of Pixels** | **Area ($km^2$)** |
|---|---|---|
| 0. Water/Goode's Interrupted Space | 52651 | 5265100 |
| 1. Evergreen Needleleaf Forest | 2327 | 232700 |
| 2. Evergreen Broadleaf Forest | 4169 | 416900 |
| 3. Deciduous Needleleaf Forest | 0 | 0 |
| 4. Deciduous Broadleaf Forest | 7027 | 702700 |
| 5. Mixed Cover | 0 | 0 |
| 6. Woodland | 197 | 19700 |
| 7. Wooded Grassland | 0 | 0 |
| 8. Closed Shrubland | 2100 | 210000 |
| 9. Open Shrubland | 4288 | 428800 |
| 10. Grassland | 15259 | 1525900 |
| 11. Cropland | 24170 | 2417000 |
| 12. Bare Ground | 9423 | 942300 |
| 13. Urban and Built-Up | 264 | 26400 |
| **Total** | 121875 | 12187500 |

The statistical analysis reveals that Deciduous Needleaf forest, mixed cover and the wooded grassland are not present in the region. Conversely, the crop land and the grassland are the dominant vegetation type over the region with total areal

coverage 2417000 $km^2$ and 1525900 $km^2$ respectively. Moreover, the deciduous forest has considerable presence with the total coverage of 702700 $km^2$.

## The land use/cover data description:

***Data Structure:***

Raster data file: 10000m. Albers conical equal area (false easting /false northing) 375x325 grid

## System files for landuse/cover data:

| *File type* | *Metadata* | *Data* |
|---|---|---|
| *Raster grid* | *Ind_lulc_UMD* | *Ind_lulc.img* |
| *Attribute Table* | *Ind_lulcl.xls* | |
| *Color Palette* | | *lulc.smp* |

### 4.3.1 Vegetation Parameters

Most of the significant vegetation parameters required for the VIC model were obtained using the vegetation parameters mapped to UMD vegetation classification scheme of the LDAS project as explained in Section 3.8.2 For each of the parameter correspond raster maps were generated. The raster data were further converted to ASCII file format, as input for the VIC Model. The elements of the datasets include architectural resistance, stomatal resistance, leaf area index,

roughness length, vegetation height, vegetation displacement height, rooting depth of the different vegetation types.

***1. Leaf Area Index (LAI)***

The raster data of 12 monthly mean LAI values were generated for each grid cell using the information from LDAS project as explained in section 3.8.2. Plate 4.13 shows the spatial variation of the dataset element for the month of June and December. The pixel distribution and the corresponding areal coverage the 12 monthly mean LAI values are listed in table 4.11. The spatial patterns of LAI in Figure 5 show good correspondence with the land cover map in Plate 4.11, with forest having the highest LAI values, and agricultural land having the lowest. Furthermore, it is evident that the LAI value tends to be the maximum in the rainy season and minimum in the winter season.

**Lai_June** **Lai_December**

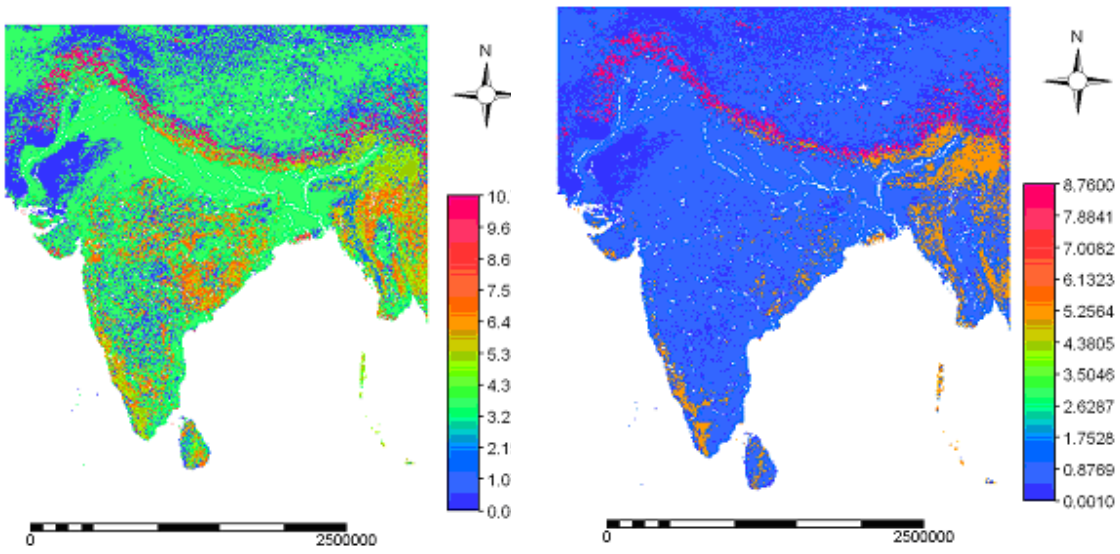


**Plate 4.13: LAI values for the month of June and December**

Plate 4.13 shows the spatial variation of the dataset element for the month of June and December. The pixel distribution and the corresponding areal coverage the 12 monthly mean LAI values are listed in table 4.11. The spatial patterns of LAI in Figure 5 show good correspondence with the land cover map in Plate 4.11, with forest having the highest LAI values, and agricultural land having the lowest. Furthermore, it is evident that the LAI value tends to be the maximum in the rainy season and minimum in the winter season.

***System Files:***

| *File type* | *Metadata* | *Data* |
|---|---|---|
| *Raster grid* | *Veg_param.doc* | *Lai_jan*<br>*Lai_feb*<br>*Lai_march*<br>.<br>.<br>*Lai_december*<br>*Lai_dec.* |
| *ASCII* | | *1.Lai_jan.asc*<br>*2.Lai_feb.asc*<br>*3.Lai_march.asc*<br>.<br>.<br>*Lai_december*<br>*12.Lai_dec. asc* |
| *Attribute Table* | *Veg_param.xls* | |

| | | |
|---|---|---|
| *Color Palette* | | *lulc.smp* |

***2. Roughness length (RL):***

Monthly raster data of Roughness length for the twelve months were generated.

**RL_June** **RL_December**

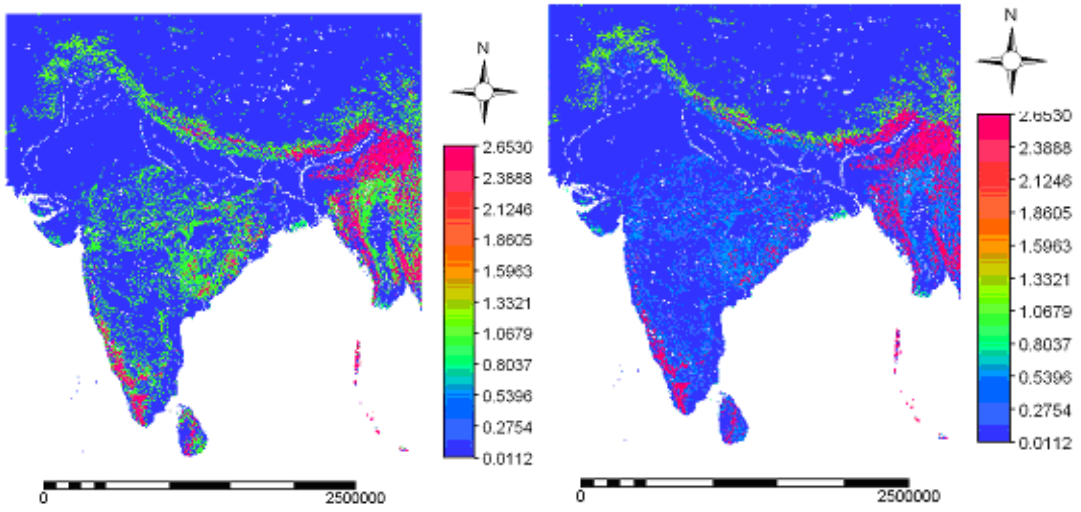


**Plate 4.14: RL values for the month of June and December**

Plate 4.14 shows the parameter variation for the month of June and December.The parameter is defined as a function of vegetation height. The pixel distribution for the value range of roughness length over the entire region is shown in Table 4.12. It shows the wide variation.

***System Files:***

| | | |
|---|---|---|
| *File type* | *Metadata* | *Data* |

| | | |
|---|---|---|
| *Raster grid* | *Veg_param.doc* | *1.RL_jan.img*<br>*2.RL_feb.img*<br>*3.RL_march.img*<br>.<br>.<br>*12.RL_dec.img* |
| *ASCII* | | *1.RL_jan.asc*<br>*2.RL_feb.asc*<br>*3.RL_march.asc*<br>.<br>.<br>*12.RL_dec. asc* |
| *Attribute Table* | *Veg_param.xls* | |
| *Color Palette* | | |

***3. Vegetation Displacement Height (VDH):***

Similarly the 12 month data for vegetation displacement height has been worked out. The parameter is also function of the vegetation height as explained in Section 3.8.2 Table 4.13 shows the spatial variation of the dataset element. Plate 4.15 shows the spatial variation of vegetation displacement height for month of June and December.

**vdh_June** **vdh_December**

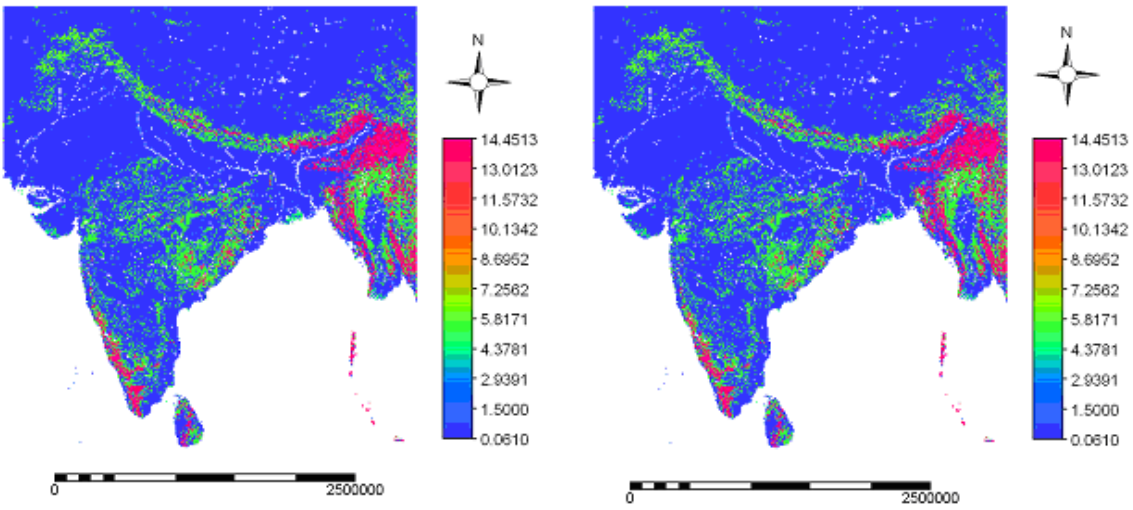


**Plate 4.15: Vegetation displacement height for June and December**

***System Files:***

| *File type* | *Metadata* | *Data(12)* |
|---|---|---|
| *Raster grid* | *Veg_param.doc* | *vdh_jan.img*<br>*vdh_feb.img*<br>*vdh_march.img*<br>.<br>.<br>*vdh_dec.img* |
| *ASCII* | | *vdh_jan.asc*<br>*vdh_feb.asc*<br>*vdh_march.asc*<br>.<br>.<br>*vdh_dec. asc* |
| *Attribute Table* | *Veg_param.doc* | |

***4. Minimum stomatal resistance (Rstom_min):***

The raster data for minimum stomatal resistance have been generated using the LDAS information. Plate 4.16 shows the spatial variation of the parameter for the

present UMD vegetation classes of the region. It is evident from the Table 4.14 that evergreen needleaf forest and the closed shrubland shows the maximum stomatal resistance i.e. 175 while the cropland shows the least i.e. 117.1.

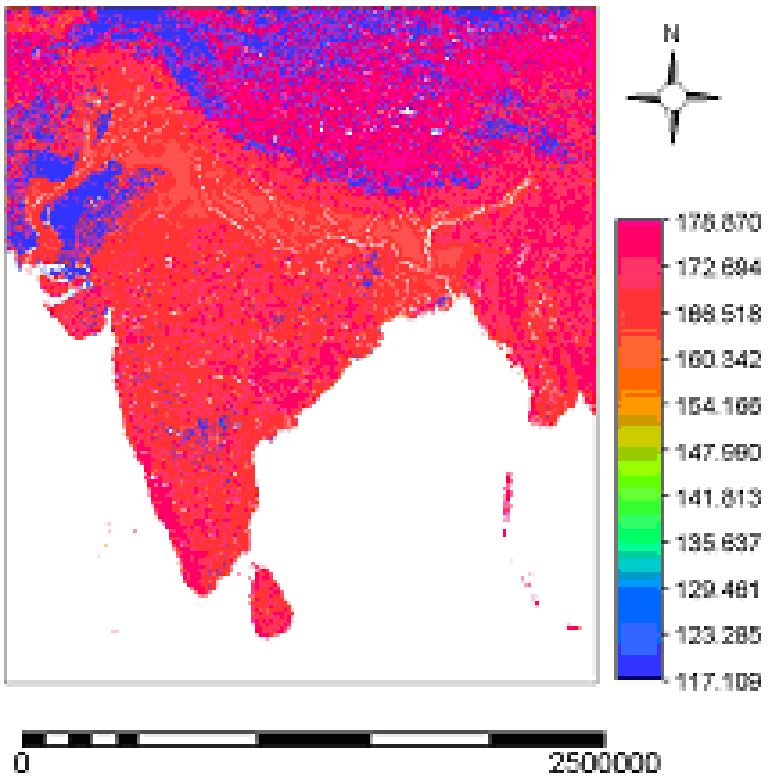


**Plate 4.16: Minimum stomatal resistance in [sec $m^{-1}$]**

**5.** ***Minimum stomatal resistance (Rstom_min)***

Architectural resistance values for UMD vegetation classes were derived based on Ducoudre *et al.* (1993). Plate 4.16 shows the spatial variation of the parameter. It's maximum for the deciduous broadleaf forest while minimum for crop land and grassland.

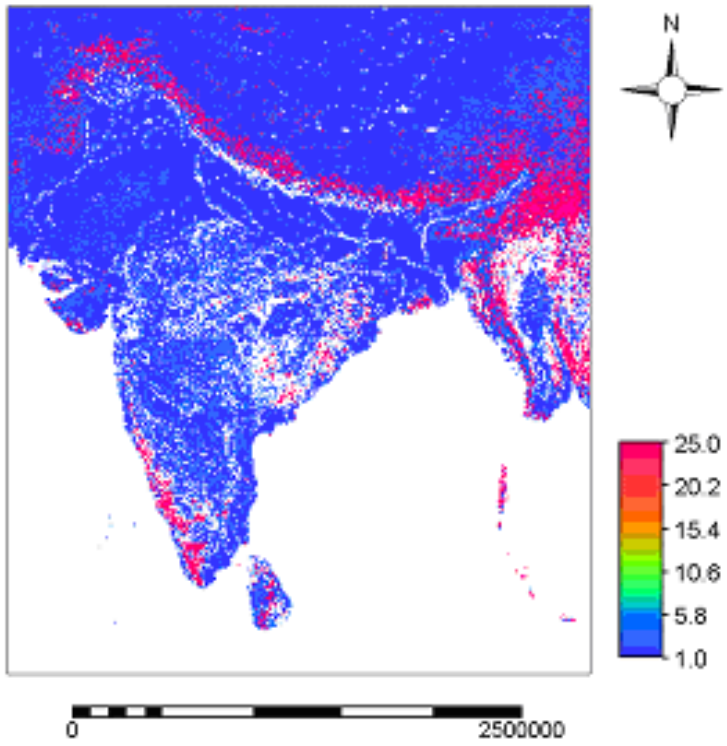


**Plate 4.17: Archtectural resistance in [sec $m^{-1}$]**

**6.** ***Minimum stomatal resistance (Rooting_depth)***

Moreover, the rooting depth values for the UMD vegetation classes have been obtained from LDAS. The spatial variation of the parameter is depicted in Table 14. The value ranges show the variation from 0.57m to 1.25 m. The evergreen and the deciduous broad leaf forest show the maximum rooting depth, while the open shrubland shows the minimum value.

***System File stomatal resistance, architectural resistance and rooting depth:***

| *File type* | *Metadata* | *Data* |
|---|---|---|
| *Raster grid* | *Veg_param.doc* | *Rstom_min.img*<br>*Archa_r.img*<br>*Rooting_depth.img* |
| *ASCII* | | *Rstom_min.asc* |

| | | |
|---|---|---|
| | | *Archa_r.asc*<br>*Rooting_depth.asc* |
| *Attribute Table* | *Veg_param.xls* | |

The important geographical information included in the documentation files (the *.doc) of the generated datasets are:

***File title*** ***: varies***

***Data type*** ***: byte or real***

***Coloumns (samples) :325***

***Rows (lines)*** ***: 375***

***Ref.system*** ***: Albers conical equal area projection***

***Ref. units*** ***: meter***

***Min. X*** ***: 863000 m.***

***Max. X*** ***: 4113000 m.***

***Min. Y*** ***: 172200 m.***

***Max. Y*** ***: 3922000 m***

***Resolution*** ***: 10000 m***

***Legend*** ***: varies***

# CHAPTER V

# SUMMARY AND CONCLUSIONS

Remote sensing and GIS have held a great deal of promise for hydrology, mainly because of the potential to observe and analyze areas and entire river basins rather than merely points. Since last decade the applied or engineering hydrology has embraced remote sensing and GIS as a useful source of data, presumably because of limitations of the traditional techniques.

With the advent of computer simulation techniques various hydrological models have been developed for hydrologic analysis. The present study is concerned with the VIC-2l model, a quasi-distributed grid based hydrologic model that parameterizes the dominant hydro-metrological processes by considering sub grid spatial variability of precipitation, infiltration and a mosaic representation of vegetation cover.

The study has compiled a new wealth of soil, vegetation and topographic information, producing digital GIS maps with attribute tables. However, the datasets are primarily applicable for VIC-2L hydrologic based land surface model at river basin level for entire India. The datasets are typically based on recent information acquired from *USGS GTOPO 30* elevation data, *MM5V3 Terrain* soil texture data, Land use/cover data of central south Asia (propriety of IIRS) and the *LDAS* project

information of NASA in addition to the information acquired from the various research work.

The methodology in the research work has been used to translate information from the global and the continental datasets into the input parameters for VIC model by utilizing the standardized procedures of image analysis and GIS interpretation. The RS/GIS softwares used in the research work included; ILWIS 3.2, ERDAS 8.6, ENVI 4.1 and Arc Map.

At the prerequisite stage of the database generation, a 10km resolution raster grid map at Albers conical equal area projection was prepared for the total of 375x325 grids, covering 12187500 $km^2$ area. The generated grid map was taken as the reference while generating the soil, vegetation and the topographic datasets.

The source data for generating the soil texture map was obtained from the 5 min. data files of the desired soil horizons (0 - 30 cm and 30 - 100 cm depths) from the downloaded directory of MM5V3/TERRAIN_DATA/, which is further based on STATSGO and FAO data source. The datasets are having 17 bands, each signifying the 17 different textural classes.

Prior to importing the scientific data sets, ENVI image headers were built, enabling the data to be viewed in ENVI. The header information included the number of samples, lines, bands (17) and interleave type (BIP).

A rough subsets corresponding to the geo-bound (60.00° to 102.00°E longitude to 0.00° to 40.00°N latitude) for each of the bands were made using the resizing program in *ENVI*. The resized data having resolution of 8 bit gray scale were saved as *ERDAS 7.5 LAN* (direct read) , which has been imported in *ERDAS*

*IMAGINE* as *(".img.)* format. *Layer stacking* in *ERDAS* enabled to georefernced by mere georeferencing of any one of its layer. Once the data has been geolocated in geographic lat/long the file coordinates corresponding to the corner position of raster grid map were worked out.

These information were later used to georeference the data files with reference to the raster grid map at Albers conical equal area projection. Finally, the data were resampled according to the desired geo-location at 10 Km grid resolution. Using the *spatial modeler* program of *ERDAS*, the 17 band data had been retransformed to single layer data. Consequently, the soil texture map for the retrospective depth of 0-30cm and 30-100cm has been generated at the model grid resolution.

The representative the soil parameters based on USDA soil texture classes estimated for the VIC model included; saturated hydraulic conductivity, soil particle density, bulk density, fraction of residual moisture content, fraction of soil moisture content at wilting point and fraction of soil moisture content at critical point and Brooks Corey exponent parameter. The estimated values were attributed in to the assimilated soil texture data of the retrospective soil depths for the corresponding raster data generation of the soil parameters at the model grid resolution. The *ASCII* format of these raster data serves as the input for the VIC model.

The land use/cover map for the study region was derived from the 45 class land use cover data of central south Asia for the vegetation dataset generation. The available data was at 1 Km grid resolution in geographic lat/long, which was initially reprojected in Albers conical projection, up scaled from 1 Km to 10 Km grid

resolution and finally recoded according to the 13 UMD vegetation classes. The values of UMD vegetation parameters required for the VIC model were obtained and derived from *table of LSM-based and observation-based vegetation parameters.* and the *Table of Mosaic-based monthly vegetation parameters which have been mapped to the UMD scheme* . *These include* stomatal resistance, leaf area index, roughness length, vegetation height, vegetation displacement height, rooting depth of the different vegetation types. The values for architectural resistance ($R_{arc}$) are based on Ducoudre *et al*. (1993). The derived values were attributed to the UMD class land use/cover data to generate the raster data of the vegetation parameters at the model grid resolution. The ASCII format of these raster data serves as the input for the VIC model.

For the topographic data generation, the DEM for the study region was derived from USGS GTOPO 30 data. The *3-dem* software was used to create multiple tertian scenes, which were saved as *".GeoTiff.* format. The data was imported in *ENVI* and using it's *mosaic program* were merged to make the cohesive image of the region having the geographic extent from 60.00° to 120.00°E longitude to 0.00° to 40.00°N latitude. The mosiacked image was finally georeferenced and resampled to make DEM at the model grid resolution. It shows the wide variation in elevation range from mere 0 m to as high as 8593m. Corresponding to the extracted DEM, slope data was derived in *Arc_Map* for each grid cell. The per cent slope shows the variation from 0 to 21.7 %. Each of the topographic data has implications in VIC river network routing model.

## CONCLUSIONS

1. The public domain geo-spatial data such as *USGS GTOPO30* and *MM5 V3 Terrain Data* can be acquired using RS/GIS software for numerous research works.
2. The freely available information obtained from the LDAS made the prodigious task of parameter acquisition for the UMD vegetation classes easier. The similar kind of approach can be used to derive the soil parameters.
3. The generated raster data for the soil and the vegetation parameters show the application of GIS and remote sensing technologies employed to integrate the non-spatial information into the spatial datasets.
4. Despite the detailed information for land cover and soil type the representative parameters are not sharply defined, as the values are merely the average estimate from the global coverage.
5. The derived datasets (soil vegetation and topography) are at the model grid resolution of 10 Km. in Albers conical equal area projection. The *ASCII* format of these datasets serves as the part of the input required to run the VIC-2L model.

# SUGGESTIONS FOR FUTURE RESEARCH WORK

- The forcing data including the monthly rainfall and temperature data files need to be generated at the same model grid resolution as generated for topography, soil and vegetation dataset.
- Some of the VIC model parameters like Albedo are quite sensitive towards the temporal and spatial variation. These region specific parameters need to be generated at the model grid resolution.
- The soil parameters like exponent of VIC curve, ARNO subsurface flow parameters including *Dsmax* parameter, *Ds* parameter and Ws parameter need to be calibrated for the specific basin.
- The VIC -2L model has to be run for each of the Indian River basins using the generated datasets of topography, soil and vegetation along with the forcing datasets; rainfall and temperature.

## 39.1.2.7.1.1.1.1 ABSTRACT

**By**

**Shashi Kant**

Hydrologists need hydrological information for watershed management planning and for making numerous analyses like predictions and forecasting. At the same time, the advent of satellite-based remote sensing and GIS along with computer simulation techniques provides a powerful tool for hydrological modeling. The Variable Infiltration Capacity (VIC) model is one of the semi-distributed, grid-based land surface models that parameterize the dominant hydro-metrological processes by considering the sub-grid variability. In the present research soil and vegetation and topographic datasets for the VIC-2L model were generated for India and part of its sub continent with the geographic extent of the region is from 65.51° to 100.65°E longitude to 2.45° to 37.45°N latitude

The datasets are typically based on recent information acquired from *USGS GTOPO 30* elevation data, *MM5V3 Terrain* soil texture data, land use/cover data of central south Asia (propriety of IIRS) and the *LDAS* project information. The digital maps of soil showing its textural classes were derived using the MM5 V3 terrain data for the two layer depths viz. 0-30cm and 30-100cm. The 45-class land cover data of south central Asia at 1km resolution was recoded to UMD vegetation classes in order to extract the LDAS information. The significant soil and vegetation parameter for the VIC model were attributed to the derived soil and land cover data for the corresponding raster data generation at the selected model grid resolution of 10x10 km in Albers conical equal area projection. The DEM for the entire region was extracted from USGS GTOPO 30 data and the corresponding per cent slope map was derived at model grid resolution. The generated data sets are defined for the 12187500 $km^2$ area having 121875 grid-cells. The ASCII files of the datasets serve as the input for the VIC-2L model.

Place:Raipur (M.P.Tripathi)

Date: Major Advisor

# BIBLIOGRAPHY


Abdulla FA, Lettenmaier D.P., Wood EF, Smith JA. (1996). Application of a macro-scale hydrologic model to estimate the water balance of the Arkansas-Red river basin. J Geophysical Research 101: 7449-4359.

Agrawal, Shefali, Joshi P. K., Yogita Shukla and Roy P. S. (2003). SPOT VEGETATION multi temporaldata for classifying vegetation in south central Asia, Current Science, Vol. 84, No. 11.

Band et al., 1991; 1993; Famiglietti and Wood, 1991; 1994; Moore and Grayson, 1991; Moore et al., 1993; Wigmosta et al., 1994; Star et al., 1997; in, http://www.epa.gov/nerlesd1/land-sci/agwa/manual/modeling.htm.(last accessed on Sep, 2005).

Barnsley, (2000). Estimation of land surface albedo and vegetation biophysical properties using SPOT-4 VGT and semi-empirical BRDF models, obtained from the website: http://vegetation.cnes.fr/vgtprep/vgt2000/ barnsley.pdf (last accessed on Sep, 2005).

Batchelor, P. (1994). Model as metaphors: the role of modelling in pollution prevention. Waste Manag., Vol. 14(3): 243-251.

Boegha, E., H. Soegaarda and Thomsen A. (2002). Evaluating evapotranspiration rates and surface conditions using Landsat TM to estimate atmospheric resistance and surface resistance, Remote Sensing of Environment 79 (2002) 329– 343.

Boer, R., P. Rakiso and Faqih A. (2000). The use of Climatic Data Generator to cope with Daily Climatic Data Scarcity in Simulation Studies, New directions for a diverse planet: Proceedings of the 4th International Crop Science Congress, Brisbane, Australia, 26 Sep – 1 Oct 2004 . Obtained from the website:http://www.cropscience. org.au/register.html (accessed on Sep, 2005.)

Brooks, R. H. and Corey A. T. (1964). Hydraulic Properties of Porous Media, Hydrology Paper 3, Colorado State University, Fort Collins, Colo.

Brown , D. and Bara, T. (1994). Recognition and Reduction of Systematic Error in Elevation and Derivative Surfaces from 7.5-Minute DEMs, Photogrammertic Engineering and Remote Sensing, Vol. 60, No. 2, p. 189-194

Burrough, P. A. (1986). Principles of geographic information systems for land resources assessment. Clarendom Press, Oxford, United Kingdom.

Burrough, P. A. (1989). Matching spatial databases and quantitative models in land resource assessment. Soil Use Manag., Vol. 5(1): 3-8.

Chakraborti, A. K. (1993). Strategies for watershed management planning using remote sensing techniques. J. of Indian Soc. of Remote Sensing-Photonirvachak, Vol. 1(2): 87-98.

Chang.D.H.and Islam S. (2000). Estimation of Soil Physical Properties Using Remote Sensing and Artificial Neural, Remote Sens. Environ. 74:534–544

Chen, J., Kumar, P. (2001). Topographic influence on the seasonal and interannual variation of water and energy balance of basins in North America. J. Clim. 14, 1989– 2014.

Cherkauer, K.A., Lettenmaier, D.P. (1999). Hydrologic effects of frozen soils in the upper Mississippi river basin. J. Geophys. Res. 104 (D16), 19599–19610.

Chow, V. T., Maidment, D. R. and Mays, L. W. (1988). Applied Hydrology, New York: McGraw-Hill.

Crawford and Linsley (1966). in, http://www.epa.gov/nerlesd1/ land-sci/agwa/manual /modeling.htm . (last accessed on May, 2005).

De Vantier, B. A. and Feldman, A. D. (1993). Review of GIS application in hydrologic modeling. J. of Water Resour. Plann. and Manag., ASCE, Vol. 119(2): 246-261.

Devito, K.J., Dillon, P.J. (1993). The influence of hydrologic con-dition and peat oxia on the phosphorus and nitrogen dynamics of a conifer swamp. Water Resour. Res. 29, 2675–2685.

Devito, K.J., Hill, A.R., Roulet, N. (1996). Groundwater–surfacewater interactions in headwater forested wetlands of the Cana-dian Shield. J. Hydrol. 181, 127–147.

Ducharne, A., Koster, R.D., Suarez, M.J., Stieglitz, M., Kumar, P. (2000). A catchment-based approach to modeling land surfaceprocesses in a general circulation model: 2. Parameter estima-tionand model demonstration. J. Geophys. Res. 105 (D20),24823– 24838.

Dümenil L, Todini E. (1992). A rainfall-runoff scheme for use in the Hamburg climate model. In Advances in Theoretical Hydrology, A Tribute to James Dooge, O'Kane JP (ed). European Geophysical Society Series on Hydrological Sciences, 1. New York: Elsevier; 129-157.

Famiglietti, J.S., Wood, E.F. (1994). Multi-scale modeling of spa-tially-variable water and energy balance processes. Water Re-sour.Res. 30, 3061– 3078.

Fleming, (1975) and Schulze (1987). Hydrological Modelling Concepts and Practice, International Institute for Infrastructural, Hydraulic and Environmental Engineering, Netherland.

Garg, P. K. (1996). Use of digital elevation model in runoff modelling. Surface Water Hydrology, V. P. Singh and B. Kumar (eds.), Kluwer Academic Pubs., Netherlands, pp.245-257.

Glover, J. (1984). Landsat feasibility study-Oklawaha basin. Prepared for the St. Johns River Water Management District, Palatka, Fla.

Greene, R. G. and Cruise, J. F. (1995). Urban watershed modeling using geographic information system. J. of Water Resour. Plann. and Manag., ASCE, Vol. 121(4): 318-325.

Haan, C. T., Johnson, H. P. and Brakensiek, D. L. (1982). Hydrological modelling of small watersheds. Pub. Am. Soc. of Agri. Engrs., 2950 Niles Road, P. O. Box 410, ASAE, St. Joseph, Michigan.

http://www.epa.gov/nerlesd1/land-sci/agwa/manual/modeling.htm (last accessed on Sep, 2005).

http://www.epa.gov/nerlesd1/land-sci/agwa/manual/modeling.htm (last accessed on Sep, 2005.)

http://www.epa.gov/nerlesd1/land-sci/agwa/manual/modeling.htm (last accessed on July, 2005.)

Jakubauskas, M. E., Whistler, J. L., Dillworth, M. E. and Martinko, E. A. (1992). Classifying remotely sensed data for use in an agricultural nonpoint source pollution model. J. of Soil and Water Cons., Vol. 47(2):179-183

Jianzhong Guo, Xu Liang and L. Ruby Leung. (2000). Impacts of different precipitation data sources on water budgets, Journal of Hydrology, Volume 298, Issues 1-4, 1, Pages 311-334).

Johnsson, K. (1994). Segment based land use classification from SPOT satellite data. Photogramm. Engg. & Remote Sensing, Vol. 60(1): 47-53.

K., Lean, J., Lettenmaier, D., Liang, X., Mahfouf, J., Men-gelkamp,H.-T., Mitchell, K., Nasonova, O., Noilhan, J., Polcher,J., Robock, A., Rosenzweig, C., Schaake, J., Schlosser, C.,Schulz, J.-P., Shao, Y., Shmakin, A., Verseghy, D., Wetzel, P.,Wood, E., Xue, Y., Yang, Z.-L., Zeng, Q., (1997). Cabauw exper-imentalresults from the project for intercomparison of land-sur-faceparameterization schemes. J. Clim. 10, 1194– 1215.

Katz, B.G., DeHan, R.S., Hirten, J.J., Catches, J.S. (1997). Interac-tions between ground water and surface water in the Suwannee river basin, Florida. J. Am. Water Resour. Assoc. 33, 1237– 1254.

Khan, M. A., V. P. Gupta and P. C. Moharana (2001). Watershed prioritization using remote sensing and geographical information system, Journal of Arid Environments (2001) 49: 465–475 available online at http://www.idealibrary.com

Koster, R.D., Suarez, M.J., Ducharne, A., Stieglitz, M., Kumar, P. (2000). A catchment-based approach to modeling land surface processes in a general circulation model: 1. Model structure.J. Geophys. Res. 105 (D20), 24809–24822.

LDAS: http://ldas.gsfc.nasa.gov( last accessed on June, 2005).

Levine, J.B., Salvucci, G.D. (1999). Equilibrium analysis of ground-water –vadose zone interactions and the resulting spatial distri-bution of hydrologic fluxes across a Canadian prairie. Water Resour. Res. 35 (5), 1369– 1383.

Liang, X., Lettenmaier, D.P., Wood, E.F. (1996a). A one-dimensional statistical dynamic representation of subgrid spatial variability of precipitation in the two-layer variable infiltration capacity model. J. Geophys. Res. 101 (D16), 21403– 21422.

Liang, X., Wood, E.F., Lettenmaier, D.P. (1996b). Surface soil mois-ture parameterization of the VIC-2L model: evaluation and modifications. Global Planet. Change 13, 195–206.

Liang, X., Lettenmaier, D.P., Wood, E.F., Burges, S.J. (1994). A simple hydrologically based model of land surface water and energy fluxes for general circulation models. J. Geophys. Res. 99 (D7), 14415–14428.

Liang, X., Wood, E.F., Lettenmaier, D.P., 1999. Modeling ground heat flux in land surface parameterization schemes. J. Geophys. Res. 104 (D8), 9581–9600.

Liang, X., Wood, E.F., Lettenmaier, D.P., Lohmann, D., Boone, A., Chang, S., Chen, F., Dai, Y., Desborough, C., Dickinson, R., Duan, Q., Ek, M., Gusev, Y., Habets, F., Irannejad, P., Koster, R., Mitchell, K., Nasonova, O., Noilhan, J., Schaake, J., Schlosser, A., Shao, Y., Shmakin, A., Verseghy, D., Warrach, K., Wetzel, P., Xue, Y., Yang, Z.-L., Zeng, Q., 1998. The project for intercomparison of land-surface parameterization schemes (PILPS) phase-2(c) Red-Arkansas River basin experiment: 2. Spatial and temporal analysis of energy fluxes. Glob. Planet. Change 19 (1 –4), 137–159 (special issue).

Liang, X., Xie, Z., (2001). A new surface runoff parameterization with subgrid-scale soil heterogeneity for land surface models. Adv. Water Resour. 24, 1173–1193.

Liang,Xu (2003). Evaluation of the effects of surface water and groundwater interactions on regional climate and local water resources, Journal of Climate:

Vol. 14, No. 8, pp. 1790 obtained from the website http://repositories.cdlib.org/wrc/tcr/liang (last accessed on May,2005).

Lilles , T. M. and R. W. Kiefer, (1994). Remote Sensing and Image Interpretation. John Wiley, New York.

Lohmann, D., Lettenmaier, D.P., Liang, X., Wood, E.F., Boone, A., Chang, S., Chen, F., Dai, Y., Desborough, C., Dickinson, R., Duan, Q., Ek, M., Gusev, Y., Habets, F., Irannejad, P., Koster, R., Mitchell, K., Nasonova, O., Noilhan, J., Schaake, J., Schlosser, A., Shao, Y., Shmakin, A., Verseghy, D., Warrach, K., Wetzel, P., Xue, Y., Yang, Z.-L., Zeng, Q., (1998). The project for intercomparison of land-surface parameterization schemes (PILPS) phase-2(c) Red-Arkansas River basin experiment: 3. Spatial and temporal analysis of water fluxes. Glob. Planet. Change 19 (1 –4), 161–179 (special issue).

Lopez, C. (1997). Locating Some Types of Random Errors in Digital Terrain Models. International Journal of Geographical InformationScience, 11(7), 677-698.

Nijssen, B., Lettenmaier, D.P., Liang, X., Wetzel, S., Wood, E.F. (1997). Streamflow simulation for continental-scale river basins. Water Resour. Res. 33 (4), 711 – 724.

Nijssen, Bart, O'Donnell, Greg M., Lettenmaier, Dennis P., Lohmann, Dag, Wood, Eric F. (2001). Predicting the Discharge of Global Rivers Journal of Climate: Vol.14, PP. 3307-3323.

Nijssen,B., R.Schnur , D.P. Lettenmaier. (2001). Global Retrospective Estimation of Soil Moisture Using the Variable Infiltration Capacity Land Surface Model. Journal of Climate: Vol. 14, No. 8, pp. 1790–1808.

NOAH: http://www.emc.ncep.noaa. (last accessed on Sep, 2005).

Olivieri, L. J., Schaal, G. M., Logan, T. J., Elliot, W. J. and Motch, B. (1991). Generating AGNPS input using remote sensing and GIS. ASAE Paper No. 91-2622, ASAE, St. Joseph, Michigan.

Opena, F. T. (1992). The application of geographic information systems to soil erosion susceptibility mapping. ASIAN-PACIFIC Remote Sensing J., Vol. 5(1): 17-122.

Peters-Lidard, C.D., Zion, M.S., Wood, E.F. (1997). A soil vegetation atmosphere transfer scheme for modeling spatially variable water and energy balance processes. J. Geophys. Res. 102, 4303–4324.

Pitman, A.J., Henderson-Sellers, A., Desborough, C., Yang, Z.-L., Abramopoulos, F., Boone, A., Dickinson, R., Gedney, N., Koster, R., Kowalczyk, E., Lettenmaier, D.P., Liang, X., Mahfouf, J.-F., Noilhan, J., Polcher, J., Qu, W., Robock, A., Rosenzweig, C.,Polidori, L., J. Chorowicz, and R. Guillande, 1991, Description of Terrain as a Fractal Surface and Application to Digital ElevationModel Quality Assessment. Photogrammetric Engineering and Remote Sensing, 57(10), 1329-1332

Rango, A. (1994). Application of remote sensing methods to hydrology and water resources. J. Hydro. Sci., Vol. 39(4): 309-319.

Rawls. (1993).., Infiltration and Soil Water Movement, In: Handbook of hydrology, D. Maidment (ed.).

Remote Sensing and GIS inputs in physically based hydrological modeling, GIS Development, http://www.gisdevelopment.net/application/nrm/water/ overview/ ato0006.htm (last accessed on Sep, 2005).

Remote Sensing and GIS inputs in physically based hydrological modeling, GIS Development,http://www.gisdevelopment.net/application/nrm/water/overview /ato0006.htm (last accessed on Sep, 2005).

Rochester, E. W., West, M. S. and Curtis, L. M. (1996). Available irrigation water from small Tennessee valley streams. Trans. of the ASAE, Vol. 39(1): 25-31.

Salvucci, G.D., Entekhabi, D. (1995). Hillslope and climatic controls on hydrologic fluxes. Water Resour. Res. 31 (7), 1725–1739.

Schaake J. (2000). Table published on the following web page: http://www.hydro.washington.edu/Lettenmaier/Models/VIC/Documentation/Info/soiltext.html (last accessed in June, 2005).

Schlosser, C.A., Shmakin, A., Smith, J., Suarez, M., Verseghy, D., Wetzel, P., Wood, E.F., Xue, Y. (1999). Key results and impli- cations from phase 1(c) of the project for intercomparison of land-surface parameterization schemes. Clim. Dyn. 15, 673– 684.

Seth, Role of Remote Sensing and GIS inputs in physically based hydrological modeling, GIS Development,http://www.gisdevelopment.net/application/ nrm/water/ overview/wato0006.htm (last accessed on August, 2005.)

Shao, Y., Henderson-Sellers, A. (1996). Validation of soil moisture simulation in land surface parameterization schemes with HA-PEX data. Glob. Planet. Change 13, 11 – 46.

Singh, V. P. (1994). Elementary Hydrology. Prentice-Hall, Englewood Cliffs, NewJersey.(http://www.epa.gov/nerlesd1/land-sci/agwa/manual/modeling. htm (last accessed on October, 2005).

Singh, V. P. (1995). Computer models of watershed hydrology, Water Resour. Publications, P.O.B. 260026, Highlands Ranch, Colorado 80126-0026, USA.

Smith, M. B. and Vidmar, A. (1994). Data set derivation for GIS based urban hydrological modelling. Photogramm. Eng. and Remote Sensing, Vol. 60(1): 67-76.

Sridhar V., Elliott L. Ronald and Lettenmaier P Dennis. (2002) Evaluation of VIC MOdel Perfoemance using Oklahoma Surface Flux Measurements American Society of Agricultural and Biology Engineering: Paper number 022132, 2002 ASAE Annual Meeting. @ 2002 www.asabe.org

system. Public Works, Vol. 125(9): 43-46.

Taylor, C.H., Pierson, D.C., 1985. The effect of a small wetland on runoff response during spring snowmelt. Atmos.-Ocean 23, 137– 154.

Theobald, D. (1989). Accuracy and Bias Issues in Surface Representation.In Goodchild, M. and S. Gopal (Eds.), The Accuracy of SpatialDatabases, (Pennsylvania: Taylor and Francis), 9, 99-106

Tim, U. S. and Jolly, R. (1994). Evaluating agricultural nonpoint source pollution using integrated geographic information systems and hydrologic water quality model. J. Environ. Qual., Vol. 23(1): 25-35.

Verry, E.S., Boelter, D.H. (1978). Peatland hydrology. In: Greeson, P.E. (Eds.), Wetland Function and Values: The State of our Understanding. American Water Resources Association, Minne-apolis, MN, pp. 389– 402.

VIC: http://www.hydro.washington.edu/Lettenmaier/Models/VIC/VIChome.html (last accessed on October, 2005)

Waddington, J.M., Roulet, N.T., Hill, A.R. (1993). Runoff mecha-nisms in a forested groundwater discharge wetland. J. Hydrol. 147, 37– 60.

Walko, R.L., Band, L.E., Baron, J., Kittel, T.G.F., Lammers, R., Lee, T.J., Ojima, D., Pielke, R.A., Taylor, C., Tague, C., Trem-back, C.J., Vidale, P.L., (2000). Coupled atmosphere bio physics hydrology models for environmental modeling. J. Appl.Meteorol. 39, 931– 944.

Wang, M. and Hjelmfelt, A. T. (1998). DEM based overland flow routing. J. Hydro. Engg., Vol. 3(1): 1-8.

Warrach, Kirsten,Stieglitz, Marc,Mengelkamp, Heinz-Theo, Raschke, Ehrhard, Warrach, Kirstern, Stieglitz, Marc, Mengelkamp, Heinz-Theo, Heinz-Theo, Raschke and Ehrhard.(2002). Advantages of a Topographically Controlled Runoff Simulation in a Soil-Vegetation Atmosphere Transfer Model. Journal of Hydrometeorology: Vol.3, issue.2, pp.131-148.

Warwick, J. J. and Haness, S. J. (1994). Efficacy of Arc/INFO GIS application to hydrologic modeling. J. of Water Resour. Plann. and Manag., ASCE, Vol. 120(3): 366-381.

Western, A.W., Grayson, R.B. (1998). The Tarrawarra data set: soil moisture patterns, soil characteristics, and hydrological flux measurements. Water Resour. Res. 34, 2765– 2768.

Whiteley, H.R., Irwin, R.W. (1986). The hydrologic response of wet lands in southern Ontario. Can. Water Resour. J. 11, 100– 110.

Wood, E.F., Lettenmaier, D.P., Liang, X., Lohmann, D., Boone, A., Chang, S., Chen, F., Dai, Y., Desborough, C., Dickinson, R., Duan, Q., Ek, M., Gusev, Y., Habets, F., Irannejad, P., Koster, R., Mitchell, K., Nasonova, O., Noilhan, J.,

Schaake, J., Schlosser, A., Shao, Y., Shmakin, A., Verseghy, D., Warrach, K., Wetzel, P., Xue, Y., Yang, Z.-L., Zeng, Q., (1998). The project for intercomparison of land-surface parameterization schemes (PILPS) phase-2(c) Red-Arkansas River basin experiment: 1. Experiment description and summary intercomparisons. Glob. Planet. Change 19 (1 – 4), 115–135 (special issue).

Wood, F., Lettenmaier, D.P., Liang, X., Nijssen, B., Wetzel, S.W. (1997). Hydrological modeling of continental-scale basins. Annu. Rev. Earth Planet. Sci. 25, 279–300.

Xie,Z.,Q.Liu and F.G.Su. (2004). An application of the VIC-3L land surface model with the new surface runoff model in simulating streamflow for the Yellow River basin, GIS and Remote Sensing in Hydrology, Water Resources and Environment (Proceedings of ICGRHWE held at the Three Gorges Dam, China, September 2003). IAHS Publ. 289, 2004

Young, R. A., Onstad, C. A., Bosch, D. D. and Anderson, W. P. (1987). AGNPS: An agricultural non-point source pollution model: A large watershed analysis tool. USDA Cons. Res. Rept. 35, pp.77.

Zhou Suoquan, Liang Xu, Chen Jing and Gong Peng. (2002). An assessment of the VIC-3L hydrological model for the Yangtze River basin based on remote sensing: a case study of the Baohe River basin The Canadian Journal of Remote sensing: http://pubs.nrc-cnr.gc.ca/cjrs/cjrs.html. (last accessed on Sep, 2005).

**Appendix A**

**Table A 1: Sample Index of Soil Hydraulic Properties***

| USDA Class | Soil Type | % Sand | % Clay | Bulk Density g/cm$^3$ | Field Capacity cm$^3$/cm$^3$ | Wilting Point cm$^3$/cm$^3$ | Porosity fraction | Saturated Hydraulic Conductivity cm/hr | Slope of Retention Curve (in log space) b** |
|---|---|---|---|---|---|---|---|---|---|
| 1 | s | 94.83 | 2.27 | 1.49 | 0.08 | 0.03 | 0.43 | 38.41 | 4.1 |
| 2 | ls | 85.23 | 6.53 | 1.52 | 0.15 | 0.06 | 0.42 | 10.87 | 3.99 |
| 3 | sl | 69.28 | 12.48 | 1.57 | 0.21 | 0.09 | 0.4 | 5.24 | 4.84 |
| 4 | sil | 19.28 | 17.11 | 1.42 | 0.32 | 0.12 | 0.46 | 3.96 | 3.79 |
| 5 | si | 4.5 | 8.3 | 1.28 | 0.28 | 0.08 | 0.52 | 8.59 | 3.05 |
| 6 | l | 41 | 20.69 | 1.49 | 0.29 | 0.14 | 0.43 | 1.97 | 5.3 |
| 7 | scl | 60.97 | 26.33 | 1.6 | 0.27 | 0.17 | 0.39 | 2.4 | 8.66 |
| 8 | sicl | 9.04 | 33.05 | 1.38 | 0.36 | 0.21 | 0.48 | 4.57 | 7.48 |
| 9 | cl | 30.08 | 33.46 | 1.43 | 0.34 | 0.21 | 0.46 | 1.77 | 8.02 |
| 10 | sc | 50.32 | 39.3 | 1.57 | 0.31 | 0.23 | 0.41 | 1.19 | 13 |
| 11 | sic | 8.18 | 44.58 | 1.35 | 0.37 | 0.25 | 0.49 | 2.95 | 9.76 |
| 12 | c | 24.71 | 52.46 | 1.39 | 0.36 | 0.27 | 0.47 | 3.18 | 12.28 |

* Source is "Average hydraulic properties of ARS soil texture classes," draft dated February, 2000 by J. Schaake. This expanded the work of others and included a total of 2128 soil samples. Wilting point is the fractional water content at 15 bar tension; field capacity is the fractional water content at 1/3 bar tension.

**b is as used in Campbell's equation. Referred by Cosby *et al* (1984).

**Table A 3: Soil parameters derived for USDA soil classes based on Table A1.**

| USDA Class | Soil Type | Bulk Density | Particle density | Diffusion Parameter | Fractioal soil moisture at critical point | Saturated Hydraulic Conductivity | Brooks Correy exponent parameter | Wilting point as a fraction of max. moisture content | Fractional residual moisture content |
|---|---|---|---|---|---|---|---|---|---|
| | | kg/m$^3$ | kg/m$^3$ | phi_s | m$^3$/m$^3$ | mm/day | | m$^3$/m$^3$ | mm$^3$/mm$^3$ |
| 1 | Sand | 1490 | 2614.04 | -0.472 | 0.43 | 9218.4 | 11.2 | 9218.4 | 0.02 |
| 2 | Loamy sand | 1520 | 2620.69 | -1.044 | 0.42 | 2608.8 | 10.98 | 2608.8 | 0.035 |
| 3 | Sandy loam | 1570 | 2616.67 | -0.569 | 0.4 | 1257.6 | 12.68 | 1257.6 | 0.041 |
| 4 | Silt loam | 1420 | 2629.63 | 0.162 | 0.46 | 950.4 | 10.58 | 950.4 | 0.027 |
| 5 | Silt | 1280 | 2666.67 | 0.162 | 0.52 | 2061.6 | 9.1 | 2061.6 | 0.02 |
| 6 | Loam | 1490 | 2614.04 | -0.327 | 0.43 | 472.8 | 13.6 | 472.8 | 0.015 |
| 7 | Sandy clay loam | 1600 | 2622.95 | -1.491 | 0.39 | 576 | 20.32 | 576 | 0.068 |
| 8 | Silty clay loam | 1380 | 2653.85 | -1.118 | 0.48 | 1096.8 | 17.96 | 1096.8 | 0.075 |
| 9 | Clay loam | 1430 | 2648.15 | -1.297 | 0.46 | 424.8 | 19.04 | 424.8 | 0.04 |
| 10 | Sandy clay | 1570 | 2661.02 | -3.209 | 0.41 | 285.6 | 5.6 | 285.6 | 0.109 |
| 11 | Siltyclay | 1350 | 2647.06 | -1.916 | 0.49 | 708 | 22.52 | 708 | 0.056 |
| 12 | Clay | 1390 | 2622.64 | -2.138 | 0.47 | 763.2 | 27.56 | 763.2 | 0.09 |

| ID.No. | Soil Type(USDA) | MMC_1(m) | MMC_2(m) | FC_1(m) | FC_2(m) | WP_1(m) | WP_2(m) | WCR_1(m) | WCR_2(m) | INT_M1(mm) | INT_M2(mm) |
|---|---|---|---|---|---|---|---|---|---|---|---|
| **1** | **sand** | 0.129 | 0.301 | 0.01032 | 0.02408 | 0.00387 | 0.00903 | 0.007224 | 0.016856 | 7.224 | 16.856 |
| **2** | **loam sand** | 0.126 | 0.294 | 0.0189 | 0.0441 | 0.00756 | 0.01764 | 0.01323 | 0.03087 | 13.23 | 30.87 |
| **3** | **sandy loam** | 0.12 | 0.28 | 0.0252 | 0.0588 | 0.0108 | 0.0252 | 0.01764 | 0.04116 | 17.64 | 41.16 |
| **4** | **silt loam** | 0.138 | 0.322 | 0.04416 | 0.10304 | 0.01656 | 0.03864 | 0.030912 | 0.072128 | 30.912 | 72.128 |
| **5** | **silt** | 0.156 | 0.364 | 0.04368 | 0.10192 | 0.01248 | 0.02912 | 0.030576 | 0.071344 | 30.576 | 71.344 |
| **6** | **loam** | 0.129 | 0.301 | 0.03741 | 0.08729 | 0.01806 | 0.04214 | 0.026187 | 0.061103 | 26.187 | 61.103 |
| **7** | **sandy clay loam** | 0.117 | 0.273 | 0.03159 | 0.07371 | 0.01989 | 0.04641 | 0.022113 | 0.051597 | 22.113 | 51.597 |
| **8** | **silty clay loam** | 0.144 | 0.336 | 0.05184 | 0.12096 | 0.03024 | 0.07056 | 0.036288 | 0.084672 | 36.288 | 84.672 |
| **9** | **clay loam** | 0.138 | 0.322 | 0.04692 | 0.10948 | 0.02898 | 0.06762 | 0.032844 | 0.076636 | 32.844 | 76.636 |
| **10** | **sandy clay** | 0.123 | 0.287 | 0.03813 | 0.08897 | 0.02829 | 0.06601 | 0.026691 | 0.062279 | 26.691 | 62.279 |
| **11** | **silty clay** | 0.147 | 0.343 | 0.05439 | 0.12691 | 0.03675 | 0.08575 | 0.038073 | 0.088837 | 38.073 | 88.837 |
| **12** | **clay** | 0.141 | 0.329 | 0.05076 | 0.11844 | 0.03807 | 0.08883 | 0.035532 | 0.082908 | 35.532 | 82.908 |

**Table A 4: The worked out Soil Parameters for the two layer depths; used for VIC Parameters estimation**

**MMC***: Maximum moisture content*
**FC**: *Field Capacity*
**WP**: *Wilting Pont*
**WCR**: *Water Content at Critical Point*
**INT_M**: *Initial Moisture Content*
**1**: *Layer Depth (0-30cm)*
**2**: *Layer Depth (30-100cm)*

Table MM5 V3

TUTORIAL

| Soil integer identification | Soil description | Max. moisture content | Reference soil moisture | Wilting poin soil moisture | Air dry moisture content | Saturation soil potential | Saturation soil conductivity (10^-6) | B parameter | Saturation soil diffusivity(10^-6) | Soil diffusion/conductive coefficient |
|---|---|---|---|---|---|---|---|---|---|---|
| **1** | **Sand** | 0.339 | 0.236 | 0.01 | 0.01 | 0.069 | 1.07 | 2.79 | 0.608 | -0.742 |
| **2** | **Loam sand** | 0.421 | 0.283 | 0.028 | 0.028 | 0.036 | 14.1 | 4.26 | 5.14 | -1.044 |
| **3** | **Sandy loam** | 0.434 | 0.312 | 0.047 | 0.047 | 0.141 | 5.23 | 4.74 | 8.05 | -0.569 |
| **4** | **Silt loam** | 0.476 | 0.36 | 0.084 | 0.084 | 0.759 | 2.81 | 5.33 | 23.9 | 0.162 |
| **5** | **Silt** | 0.476 | 0.36 | 0.084 | 0.084 | 0.759 | 2.81 | 5.33 | 23.9 | 0.162 |
| **6** | **Loam** | 0.439 | 0.329 | 0.066 | 0.066 | 0.355 | 3.38 | 5.25 | 14.3 | -0.327 |
| **7** | **Sandy clay loam** | 0.404 | 0.314 | 0.067 | 0.067 | 0.135 | 4.45 | 6.66 | 9.9 | -1.491 |
| **8** | **Silty clay loam** | 0.464 | 0.387 | 0.12 | 0.12 | 0.617 | 2.04 | 8.72 | 23.7 | -1.118 |
| **9** | **Clay loam** | 0.465 | 0.382 | 0.0103 | 0.0103 | 0.263 | 2.45 | 8.17 | 11.3 | -1.297 |
| **10** | **Sandy clay** | 0.406 | 0.338 | 0.1 | 0.1 | 0.098 | 7.22 | 10.73 | 18.7 | -3.209 |
| **11** | **Silty clay** | 0.468 | 0.404 | 0.126 | 0.126 | 324 | 1.34 | 10.39 | 9.64 | -1.916 |
| **12** | **Cay** | 0.468 | 0.412 | 0.138 | 0.138 | 0.468 | 0.974 | 11.55 | 11.2 | -2.138 |
| **13** | **Organic material** | 0.439 | 0.329 | 0.066 | 0.066 | 0.355 | 3.38 | 5.25 | 14.3 | -0.327 |
| **14** | **Water** | 1 | 0 | 0 | 0 | 0 | 0 | 0 | 0 | 0 |
| **15** | **Bed rock** | 0.2 | 0.108 | 0.006 | 0.006 | 0.069 | 141 | 2.79 | 136 | -1.111 |
| **16** | **Other** | 0.421 | 0.283 | 0.028 | 0.028 | 0.036 | 14.1 | 7.26 | 5.14 | -1.044 |
| **17** | **No data** | | | | | | | | | |

| | | bulk density(g/cm ^3) | Field capacity (cm^3/cm^3)* | Wilting Point(cm3/cm3) | POROSITY FRACTION | saturated hydraulic conductivity(cm/hr) | slope of retention curve( in log space)b** |
|---|---|---|---|---|---|---|---|
| 1 | **Sand** | 1.49 | 0.08 | 0.03 | 0.43 | 38.41 | 4.1 |
| 2 | **Loam sand** | 1.52 | 0.15 | 0.06 | 0.42 | 10.87 | 3.99 |
| 3 | **Sandy loam** | 157 | 0.21 | 0.09 | 0.4 | 5.24 | 4.84 |
| 4 | **Silt loam** | 1.42 | 0.32 | 0.12 | 0.46 | 3.96 | 3.79 |
| 5 | **Silt** | 1.28 | 0.28 | 0.08 | 0.52 | 8.59 | 3.05 |
| 6 | **Loam** | 1.49 | 0.29 | 0.14 | 0.43 | 1.97 | 5.3 |
| 7 | **Sandy clay loam** | 1.6 | 0.27 | 0.17 | 0.39 | 2.4 | 8.66 |
| 8 | **Silty clay loam** | 1.38 | 0.36 | 0.21 | 0.48 | 4.57 | 7.48 |
| 9 | **Clay loam** | 1.43 | 0.34 | 0.21 | 0.46 | 1.77 | 8.02 |
| 10 | **Sandy clay** | 1.57 | 0.31 | 0.23 | 0.41 | 1.19 | 1.3 |
| 11 | **Silty clay** | 1.35 | 0.37 | 0.25 | 0.49 | 2.95 | 9.76 |
| 12 | **Cay** | 1.39 | 0.36 | 0.27 | 0.47 | 3.18 | 12.28 |

| UMD Vegetation Classes | No. of Pixels | Area (km2) | LAI_Jan | LAI_Feb | LAI_March | LAI_April | LAI_May | LAI_June | LAI_July | LAI_Aug |
|---|---|---|---|---|---|---|---|---|---|---|
| | | | | | | | | | | |
| **1. Evergreen Needleleaf Forest** | 2327 | 232700 | 8.76 | 9.16 | 9.827 | 10.93 | 10.36 | 10.76 | 10.493 | |
| **2. Evergreen Broadleaf Forest** | 4169 | 416900 | 5.117 | 5.117 | 5.117 | 5.117 | 5.117 | 5.117 | 5.117 | |
| **3. Deciduous Broadleaf Forest** | 7027 | 702700 | 0.52 | 0.52 | 0.867 | 2.107 | 4.507 | 6.773 | 7.173 | |
| **4. Woodland** | 197 | 19700 | 5.27 | 5.52859 | 6.006 | 6.442 | 7.244 | 8.363 | 8.54 | |
| **5. Closed Shrubland** | 2100 | 210000 | 0.58055 | 0.629 | 0.6285 | 0.6285 | 0.919 | 1.768 | 2.55 | |
| **6. Open Shrubland** | 4288 | 428800 | 0.399 | 0.404 | 0.3138 | 0.223 | 0.249 | 0.33 | 0.432 | |
| **7. Grassland** | 15259 | 1525900 | 0.782 | 0.893 | 1.004 | 1.116 | 1.782 | 3.671 | 4.782 | |
| **8. Cropland** | 24170 | 2417000 | 0.782 | 0.893 | 1.004 | 1.116 | 1.78 | 3.671 | 4.782 | |
| **9. Bare Ground** | 9423 | 942300 | 0.001 | 0.001 | 0.001 | 0.001 | 0.001 | 0.001 | 0.001 | |
| **10. Urban and Built-Up** | 264 | 26400 | 1.286 | 1.394 | 1.55069 | 2.519 | 2.519 | 4.136 | 5.021 | |
| | **69224** | **6922400** | | | | | | | | |

| UMD Vegetation Classes | No. of Pixels | VDH_Jan | VDH_Feb | VDH_March | VDH_April | VDH_May | VDH_June | VDH_July | VDH_Aug | VDH_Sep |
|---|---|---|---|---|---|---|---|---|---|---|
| **1. Evergreen Needleleaf Forest** | 2327 | 6.057236 | 6.008211 | 5.926504 | 5.8938211 | 5.861138 | 5.817561 | 5.844797 | 5.8774797 | 5.8938 |
| **2. Evergreen Broadleaf Forest** | 4169 | 14.4513 | 14.4513 | 14.4513 | 14.451301 | 14.4513 | 14.4513 | 14.4513 | 14.451301 | 14.45 |
| **4. Deciduous Broadleaf Forest** | 7027 | 2.83252 | 2.83252 | 3.627805 | 4.9569106 | 5.616016 | 5.686829 | 5.675935 | 5.6486992 | 5.6432 |
| **6. Woodland** | 197 | 4.139837 | 4.113378 | 4.232439 | 4.49397 | 4.608293 | 4.602301 | 4.61374 | 4.6246341 | 4.6377 |
| **8. Closed Shrubland** | 2100 | 0.30722 | 0.30722 | 0.302317 | 0.2952358 | 0.295236 | 0.293602 | 0.291967 | 0.3104878 | 0.3208 |
| **9. Open Shrubland** | 4288 | 0.201 | 0.201 | 0.19174 | 0.178122 | 0.178122 | 0.178122 | 0.174309 | 0.212439 | 0.2255 |
| **10. Grassland** | 15259 | 0.423244 | 0.423789 | 0.423789 | 0.4243333 | 0.423789 | 0.419976 | 0.413439 | 0.417252 | 0.4237 |
| **11. Cropland** | 24170 | 0.423244 | 0.423789 | 0.423789 | 0.4243333 | 0.423789 | 0.419976 | 0.413439 | 0.417252 | 0.4237 |
| **12. Bare Ground** | 9423 | 0.061008 | 0.061008 | 0.061008 | 0.0610081 | 0.061008 | 0.061008 | 0.061008 | 0.0610081 | 0.0610 |
| **13. Urban and Built-Up** | 264 | 1.060561 | 1.057293 | 1.133008 | 1.2713659 | 1.338366 | 1.34 | 1.336187 | 1.3416341 | 1.3476 |
| | | | | | | | | | | |

| UMD Vegetation Classes | No. of Pixels | Area ($km^2$) | Overstory | Architectural Resistance [sec m-1] | Minimum Stomatal Resistance [sec m-1] |
|---|---|---|---|---|---|
| **1. Evergreen Needleleaf Forest** | 2327 | 232700 | 1 | 25 | 175 |
| **2. Evergreen Broadleaf Forest** | 4169 | 416900 | 1 | 25 | 150 |
| **3. Deciduous Broadleaf Forest** | 7027 | 702700 | 1 | 40 | 175 |
| **4. Woodland** | 197 | 19700 | 1 | 20 | 173.51 |
| **5. Closed Shrubland** | 2100 | 210000 | 1 | 3 | 175 |
| **6. Open Shrubland** | 4288 | 428800 | 1 | 3 | 178.87 |
| **7. Grassland** | 15259 | 1525900 | 0 | 2 | 165 |
| **8. Cropland** | 24170 | 2417000 | 0 | 2 | 117.1085 |
| **9. Bare Ground** | 9423 | 942300 | 0 | 1 | 175 |
| **10. Urban and Built-Up** | 264 | 26400 | 1 | 1 | 154.84 |
| **Total** | **69224** | **6922400** | | | |